Article

Cell

Degradation of Phage Transcripts by CRISPR-Associated RNases Enables Type III CRISPR-Cas Immunity

Graphical Abstract

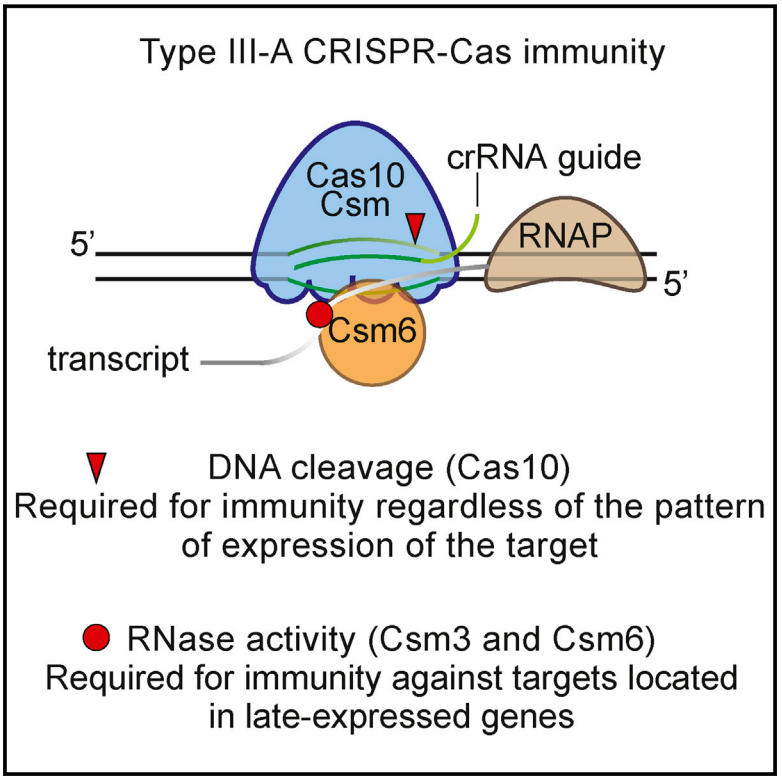

Highlights

- Target transcription is required for anti-viral type III CRISPR-Cas immunity
- Targets in late-expressed genes delay immunity allowing the accumulation of viral DNA
- The Csm3 and Csm6 CRISPR RNases degrade viral transcripts
- Transcript degradation enables immunity when targets are in late-expressed genes

Authors

Wenyan Jiang, Poulami Samai, Luciano A. Marraffini

Correspondence

marraffini@rockefeller.edu

In Brief

RNA-guided DNA cleavage is often sufficient to protect bacteria against infections by DNA viruses. However, cleavage of viral transcripts is required for type III CRISPR-Cas immunity when the target is located in a late-expressed gene or when there are mismatches between the RNA guide and the target DNA.

Jiang et al., 2016, Cell *164*, 710–721
February 11, 2016
http://dx.doi.org/10.1016/j.cell.2015.12.053

CellPress

Cell

Article

Degradation of Phage Transcripts by CRISPR-Associated RNases Enables Type III CRISPR-Cas Immunity

Wenyan Jiang,[1] Poulami Samai,[1] and Luciano A. Marraffini[1,*]
[1]Laboratory of Bacteriology, The Rockefeller University, 1230 York Avenue, New York, NY 10065, USA
*Correspondence: marraffini@rockefeller.edu
http://dx.doi.org/10.1016/j.cell.2015.12.053

SUMMARY

Type III-A CRISPR-Cas systems defend prokaryotes against viral infection using CRISPR RNA (crRNA)-guided nucleases that perform co-transcriptional cleavage of the viral target DNA and its transcripts. Whereas DNA cleavage is essential for immunity, the function of RNA targeting is unknown. Here, we show that transcription-dependent targeting results in a sharp increase of viral genomes in the host cell when the target is located in a late-expressed phage gene. In this targeting condition, mutations in the active sites of the type III-A RNases Csm3 and Csm6 lead to the accumulation of the target phage mRNA and abrogate immunity. Csm6 is also required to provide defense in the presence of mutated phage targets, when DNA cleavage efficiency is reduced. Our results show that the degradation of phage transcripts by CRISPR-associated RNases ensures robust immunity in situations that lead to a slow clearance of the target DNA.

INTRODUCTION

Clustered, regularly interspaced, short, palindromic repeats (CRISPR) loci and their associated (*cas*) genes encode an adaptive immune system that protects bacteria and archaea from viral (phage) and plasmid infection (Barrangou et al., 2007; Marraffini and Sontheimer, 2008). The targets of immunity are specified by short spacer sequences that intercalate in between the CRISPR repeats (Bolotin et al., 2005; Mojica et al., 2005; Pourcel et al., 2005). New spacers are acquired during infection (Barrangou et al., 2007) from all regions of the invader's genome (Datsenko et al., 2012; Heler et al., 2015; Paez-Espino et al., 2013) and are inserted into the CRISPR array by the Cas1-Cas2 complex (Arslan et al., 2014; Nuñez et al., 2014, 2015; Yosef et al., 2012). Each spacer sequence is transcribed and processed into a small antisense RNA (Brouns et al., 2008; Carte et al., 2008; Deltcheva et al., 2011), the CRISPR RNA (crRNA), which associates with RNA-guided Cas nucleases to specify a matching target in the genome of the invading phage or plasmid (Gasiunas et al., 2012; Jinek et al., 2012; Samai et al., 2015; Westra et al., 2012). It is believed that cleavage of the foreign DNA destroys the genetic material of the invader and stops the infection (Garneau et al., 2010).

Based on their *cas* gene content, CRISPR-Cas systems can be classified into five types: I–V (Makarova et al., 2015). Type III CRISPR-Cas systems display an elaborate targeting mechanism mediated by the Cas10-Csm (type III-A) or the Cas10-Cmr (type III-B) complexes. Transcription of the target sequence is required for immunity (Deng et al., 2013; Goldberg et al., 2014) and for the cleavage of the non-template strand of the target DNA (Samai et al., 2015). Type III Cas10 complexes are also capable of crRNA-guided RNA cleavage (Hale et al., 2009; Samai et al., 2015; Staals et al., 2014; Tamulaitis et al., 2014; Zhang et al., 2012). In the Cas10-Csm complex, conserved aspartate residues within the palm domain of Cas10 are required for DNA cleavage (Samai et al., 2015), and Csm3 contains the crRNA-guided RNase activity (Samai et al., 2015; Staals et al., 2014; Tamulaitis et al., 2014). These activities result in the co-transcriptional cleavage of the target DNA and its transcripts (Samai et al., 2015). While DNA targeting is essential for the clearance of foreign plasmids and DNA phages (Goldberg et al., 2014; Marraffini and Sontheimer, 2008; Samai et al., 2015), a role for transcript cleavage during immunity against these DNA elements has not been determined.

In addition to the Cas10 complexes, type III CRISPR-Cas loci code for Csm6 or Csx1 (Makarova et al., 2011b), proteins that contain a Higher Eukaryotes and Prokaryotes Nucleotide-binding (HEPN) domain (Anantharaman et al., 2013). Bioinformatic analysis of Csm6 and Csx1 suggested that they function as metal-independent RNases (Anantharaman et al., 2013). In *Staphylococcus epidermidis*, deletion of *csm6* results in the disruption of type III-A CRISPR-Cas immunity against conjugative plasmids (Hatoum-Aslan et al., 2014). Since absence of Csm6 does not affect the biogenesis of crRNAs, it has been proposed that this protein participates in the targeting of nucleic acids. However, Csm6 is not part of the Cas10-Csm complex that cleaves DNA molecules in vitro (Hatoum-Aslan et al., 2013; Samai et al., 2015; Staals et al., 2014; Tamulaitis et al., 2014), and its precise role in type III CRISPR-Cas immunity has not been explored.

We studied the role of RNA targeting for the type III-A CRISPR-Cas system of *S. epidermidis*. We first determined that Csm6 is an RNase not required for the destruction of the target DNA. We then explored the contribution of both RNases of this system, Csm3 and Csm6, to CRISPR immunity during phage infection. We show that transcription-dependent targeting results in a

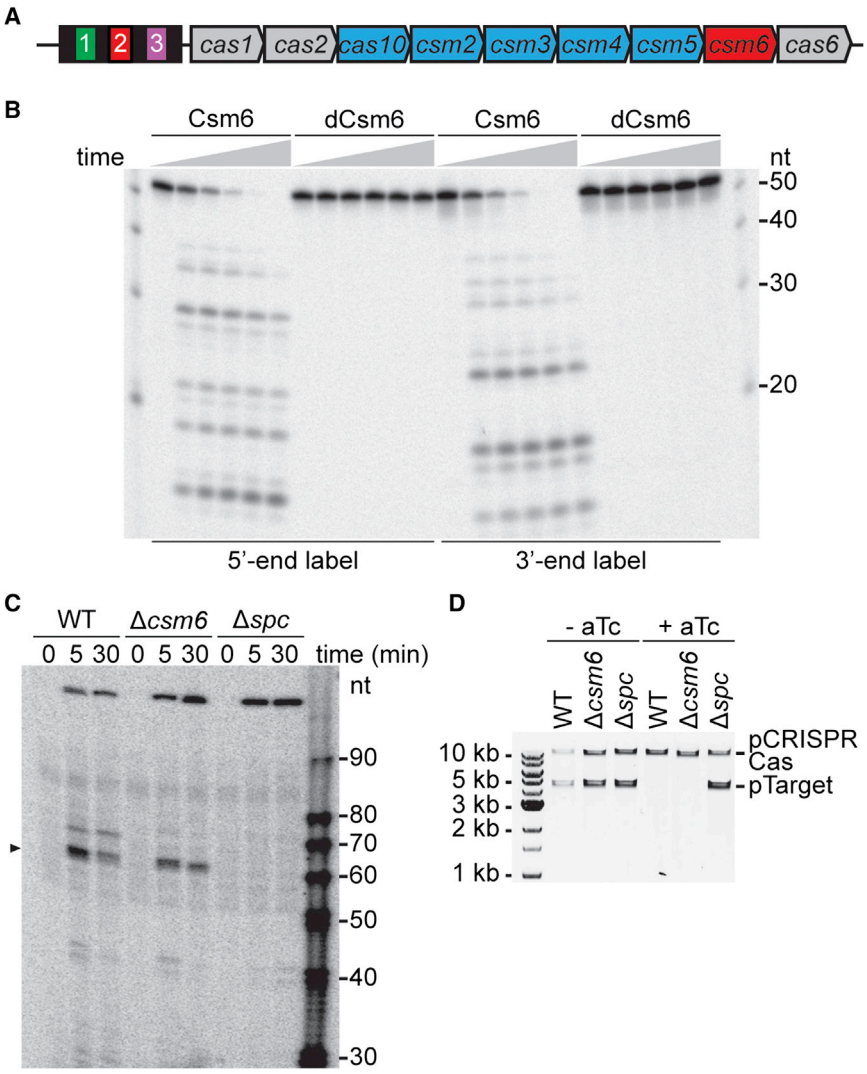

Figure 1. Csm6 Is an RNase Not Involved in Type III-A DNA Degradation

(A) *S. epidermidis* RP62a carries a type III-A CRISPR-Cas locus that harbors four repeats (black boxes), three spacers (colored boxes), and nine *cas/csm* genes. *cas10* and *csm2-5* (in blue) encode for the Cas10-Csm ribonucleoprotein complex that has crRNA-guided DNA and RNA cleavage activities. The function of *csm6* (in red) is unknown.

(B) Purified Csm6 and dCsm6 were incubated with a radiolabeled ssRNA substrate. The reaction proceeded for 1 hr and aliquots were taken at 0, 5, 15, 30, 45, and 60 min for PAGE and phosphorimager visualization.

(C) A 5′-radiolabeled primer is used to initiate reverse transcription of the target transcript, generating a 171-nt extension product in the absence of RNA cleavage. The target is located in the pTarget plasmid under the control of a tetracycline-inducible promoter; this plasmid was introduced in different strains carrying the wild-type, Δ*csm6*, or Δ*spc* (non-targeting control) CRISPR-Cas systems. Total RNA for primer extension was extracted at different times after addition of the aTc transcription inducer. Primer extension products were separated by PAGE and detected by phosphorimaging; the products indicating transcript cleavage are marked with an arrowhead.

(D) pTarget plasmid DNA was extracted from cells before and after 10 hr of treatment with aTc, testing the different CRISPR-Cas backgrounds described in (C).

See also Figure S1.

sharp increase of viral genomes in the host cell when the target is located in a late-expressed phage gene. In this targeting condition, mutations in the active sites of the type III-A RNases Csm3 and Csm6 lead to the accumulation of the target phage mRNA and abrogate immunity. Csm6 is also required to provide defense in the presence of mutated phage targets, when DNA cleavage efficiency is reduced. Our results show that the degradation of phage transcripts by CRISPR-associated RNases ensures robust immunity in situations that lead to a slow clearance of the target DNA.

RESULTS

Csm6 Is an RNase Not Involved in Type III-A DNA Degradation

The type III-A CRISPR-Cas system of *S. epidermidis* harbors nine *cas* genes (Figure 1A). *cas1* and *cas2* are present in most CRISPR-Cas systems and form a complex responsible for the integration of new spacers into the CRISPR array (Arslan et al., 2014; Nuñez et al., 2015; Yosef et al., 2012). *cas6* encodes for an endoribonuclease that processes the crRNA precursor into small crRNA guides in both type I (Brouns et al., 2008) and type III (Carte et al., 2008) systems. *cas10*, along with *csm2*, *csm3*, *csm4*, and *csm5*, encode a ribonucleoprotein complex characteristic of type III-A systems known as the Cas10-Csm complex (Hatoum-Aslan et al., 2013; Staals et al., 2014; Tamulaitis et al., 2014). *csm6* is the only gene that has not been characterized in detail. A recent bioinformatics study of the HEPN family indicated that Csm6 is a member of this group and may function as metal-independent RNase (Anantharaman et al., 2013). To investigate this, we expressed Csm6 in *Escherichia coli* and purified it to homogeneity, along with the putative active site double mutant R364A,H369A ($Csm6^{R364A,H369A}$ or "dead" Csm6, dCsm6). Incubation of Csm6 with single-stranded RNAs (ssRNAs) radiolabeled at either end resulted in the degradation of the substrate by the wild-type Csm6, but not the active site double mutant (Figure 1B). The reaction did not require any metal ion (Mg, Mn, and EDTA were tested and obtained the same cleavage; data not shown). We obtained similar results with the individual mutants (Figure S1A), using substrates of different sequences and lengths (Figure S1B). Therefore, these results confirm that Csm6 is a metal-independent,

sequence-independent RNase. The Cas10-Csm complex also contains crRNA-guided RNase activity within the Csm3 subunit (Samai et al., 2015; Staals et al., 2014; Tamulaitis et al., 2014). To test whether Csm6 RNase activity influences the RNA cleavage activity of the Cas10-Csm complex, we looked at the cleavage of target transcripts in vivo, using a previously developed primer extension assay (Samai et al., 2015) (Figure S1C). We looked at the transcript cleavage products generated by the Cas10-Csm complex in strains carrying a wild-type, Δ*csm6*, or Δ*spc1* CRISPR-Cas system (Figure 1C). No cleavage was detected in the absence of the *spc1* crRNA guide, and the same Csm3-dependent transcript cleavage product was detected in wild-type and Δ*csm6* strains. These results indicate that the Csm6 RNase activity does not influence the crRNA-guided transcript cleavage performed by the Csm3 subunit of the Cas10-Csm complex.

Genetic characterization of the *S. epidermidis* CRISPR-Cas system indicated that *csm6* is required for immunity against plasmid conjugation (Hatoum-Aslan et al., 2014). Since DNA targeting is required for this immunity (Marraffini and Sontheimer, 2008), it was proposed that Csm6 could participate in the degradation of plasmid DNA. To test this, we looked at the stability of the pTarget plasmid upon induction of target transcription with anhydrotetracycline (aTc) in different genetic backgrounds (Figure 1D). The plasmid was stable in the absence of the *spc1* crRNA and was equally degraded by the wild-type and Δ*csm6* CRISPR-Cas systems. Corroborating this finding, we determined that *csm6* is not required for targeting of chromosomal DNA (Figures S1D and S1E). Finally, we tested the activity of Csm6 against single-stranded DNA (ssDNA) and double-stranded DNA (dsDNA) substrates in vitro but failed to obtain any cleavage products (Figure S1F). Altogether, these results demonstrate that the RNase activity of Csm6 is not involved in DNA targeting.

Csm3 and Csm6 Are Required for the Degradation of Phage Transcripts

Together with previous reports, the above results show that the *S. epidermidis* type III-A CRISPR-Cas system encodes for two RNases: a sequence-specific, crRNA-guided endoribonuclease, Csm3, and another, crRNA-independent ribonuclease, Csm6. To determine the role of these RNases in anti-viral immunity, we explored their effect on phage transcripts during infection. To do this, we transformed *Staphylococcus aureus* cells with different pCRISPR-Cas constructs (Hatoum-Aslan et al., 2013) and infected them with the staphylococcal lytic phage ΦNM1γ6 (Goldberg et al., 2014). Transcriptome analysis of *S. aureus* cells infected with ΦNM1γ6 in the absence of CRISPR-Cas immunity showed a gradual accumulation of transcripts after infection, with transcription of the first 12 kb of the genome during the first 15 min post-infection and requiring 30 min for the expression of the full set of lytic genes (Goldberg et al., 2014). At different times post-infection, we extracted total RNA and measured the abundance of phage transcripts during type III-A CRISPR-Cas immunity in the presence or absence of Csm3 and/or Csm6 RNase activity using qRT-PCR. First, we quantified phage RNA accumulation during the targeting of an early-transcribed gene, *gp14* (encoding a protein involved in phage DNA replication), with primers that amplify the targeted region (~100 bp flanking the target sequence defined by the crRNA) at 15, 45, and 90 min post-infection (Figure 2A). We compared a wild-type CRISPR-Cas system, a non-targeting control lacking the matching spacer sequence (Δ*spc*), and systems lacking Csm3 RNase activity (*csm3*^{D32A} or "dead" *csm3*, d*csm3*) (Samai et al., 2015), Csm6 RNase activity (*csm6*^{R364A,H369A} or d*csm6*), or both (Figure 2B). Transcript accumulation was minimal during *gp14* targeting in the wild-type strain and increased dramatically in the absence of immunity, approximately a 130-fold increase at the 45-min time point (0.6 for wild-type versus 83 for Δ*spc*). We did not detect any substantial accumulation of phage transcripts in the d*csm6*, d*csm3*, or d*csm3*/d*csm6* strains. When we performed the same experiment but targeting the late-transcribed *gp43* gene (encoding a phage capsid subunit), we observed minor differences between target transcript accumulation in wild-type, d*csm3*, and d*csm6* strains (Figure 2C). However, we detected a significant increase in viral transcripts in the d*csm3*/d*csm6* double mutant, which accumulated similar levels of phage mRNA as infected cells that lack CRISPR-Cas immunity (Δ*spc*) 45 min after infection. At 90 min post-infection, we detected a 2-fold increase in the *gp43* transcript level in Δ*spc* cells compared to the d*csm3*/d*csm6* double mutant, which is likely due to the presence of DNA cleavage and less phage propagation in the latter. We also performed RNA deep sequencing (RNA-seq) in infected cells with different genetic backgrounds. The results confirm the qRT-PCR data, showing that *gp14* phage transcripts are not accumulated during the immune response of the different CRISPR-Cas systems (Figure 2D), but that there is a substantial increase in *gp43* transcript levels (similar to the Δ*spc* control) in the d*csm3*/d*csm6* double mutant at 45 min post-infection (Figure 2E). Together, these results indicate that the RNase activity of either Csm3 or Csm6 is required to prevent the accumulation of phage transcripts when the type III-A CRISPR-Cas system targets late-, but not early-, expressed genes.

We also wanted to investigate the specificity of the RNase activity of Csm3 and Csm6 described above. We found no *csm3*- or *csm6*-specific degradation of the plasmid-born *cat* gene transcript (Figure S2A) nor of the chromosomally expressed *fabD* and *glyA* mRNAs (Figure S2B). In addition, overexpression of Csm6 did not result in a cell growth defect (Figure S2C), which would be expected for a non-specific RNase. On the other hand, the specific degradation of phage transcripts extended for at least 1 kb at each side of the target site defined by the crRNA guide (Figure S2E). RNA-seq of phage transcripts in wild-type, d*csm3*, d*csm6*, or d*csm3*/d*csm6* cells corroborated these results (Figure S2F). In addition, it showed that there is a very low level of phage transcripts from sequences flanking the target region in d*csm3* cells, indistinguishable to the transcript levels of wild-type cells. However, an increased accumulation (similar to the Δ*spc* control in the *gp42* and *gp52* regions) was observed for the d*csm6* mutant. These data suggest that Csm6, and not Csm3, is responsible for much of the transcript degradation outside of the target region. The mechanism by which the RNase activity of Csm6 is first localized to the Cas10-Csm transcript target remains to be elucidated.

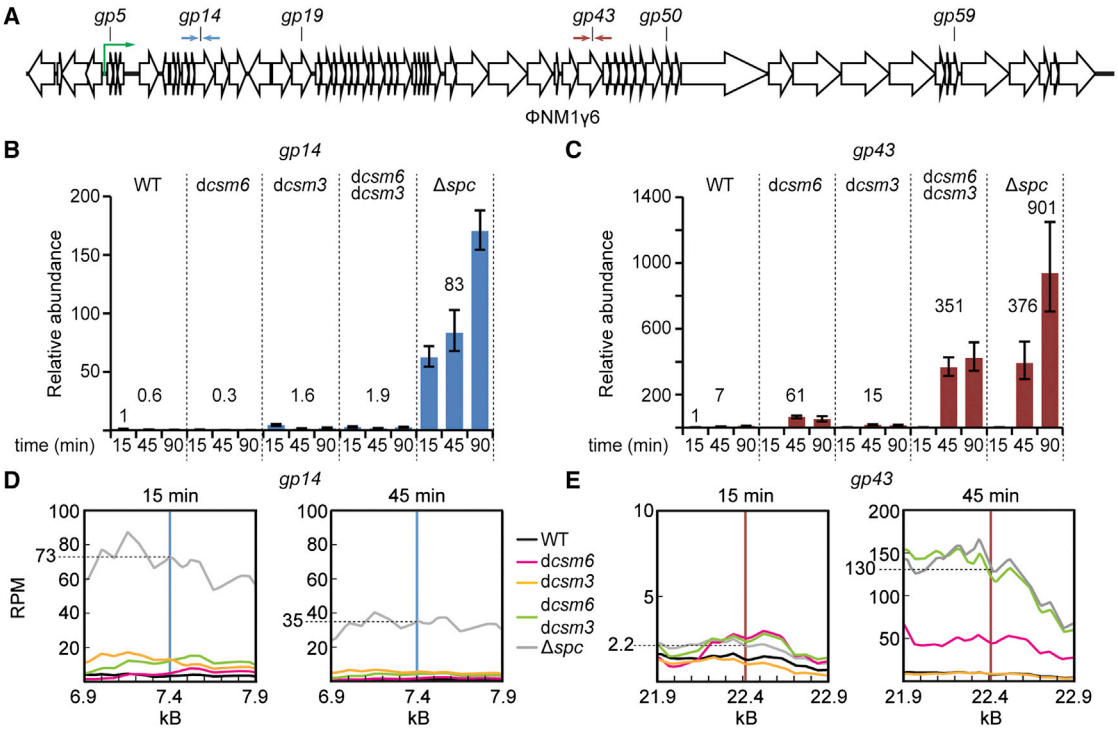

Figure 2. Csm3 and Csm6 Are Required for the Degradation of Phage Transcripts

(A) Schematic diagram of the ΦNM1γ6 genome in its linear (prophage) form and the position of type III-A CRISPR-Cas targets used in this study. Table S1 contains the full sequence of each target. The green arrow represents the rightward promoter driving transcription of the lytic genes and defines the early expressed genes as those immediately downstream of this promoter. During the lytic cycle, the genome is circular. The opposed arrows indicate the primers used for qRT-PCR experiments in (B) and (C).

(B) qRT-PCR performed on the ΦNM1γ6 *gp14* transcript using total RNA collected at different times post-infection from cells carrying different type III-A CRISPR-Cas systems targeting the *gp14* gene. Values for the *rho* gene were used for normalization. The normalized value for the measurement at 15 min in wild-type cells was set to 1 to obtain the relative abundance of the *gp14* transcript for the rest of the data points (mean ± SD of four replicas).

(C) Same as (B), but using CRISPR-Cas systems targeting the ΦNM1γ6 *gp43* gene and measuring relative abundance of the *gp43* transcript.

(D) RNA-seq reads (reads per 500 bases of transcript per million mapped reads, RPM) for transcripts in the vicinity of the *gp14* target at 15 and 45 min post-infection of cells harboring different mutations in the type III-A CRISPR-Cas system. Vertical blue line indicates target position.

(E) Same as (D), but showing transcription levels in the *gp43* target region.

See also Figure S2.

Co-transcriptional Type III CRISPR-Cas Targeting Leads to the Accumulation of Phage DNA

The transcription requirement for DNA cleavage of type III CRISPR-Cas systems implies that when a late-expressed gene is targeted, the phage infection cycle will proceed unchecked until the target is transcribed. This can take 15–30 min (Goldberg et al., 2014) and would allow the accumulation of both phage DNA and RNA that results from virus replication and transcription, respectively. Figure 2 shows that the type III-A RNases Csm3 or Csm6 prevent the accumulation of phage transcripts in this scenario, i.e., when the late-expressed gene *gp43* is targeted; in Figure 3, we investigated the fate of phage DNA during type III-A CRISPR-Cas immunity. First, we performed southern blot analysis on cells infected with ΦNM1γ6 carrying different CRISPR-Cas systems targeting *gp43* (Figure 3A). As controls, we looked at phage DNA in cells carrying a type II CRISPR-Cas system that targets *gp43* (Goldberg et al., 2014) and in cells without CRISPR-Cas immunity. The expected 3.9-kb band that results from restriction digestion of the target site (Figure 3A) was minimally detected in the presence of type II immunity (Figure 3B). This is in agreement with previous findings that showed that phage DNA is immediately degraded upon injection by the type II Cas9 crRNA-guided nuclease (Garneau et al., 2010), which does not require target transcription for DNA cleavage (Gasiunas et al., 2012; Jinek et al., 2012). In cells with type III-A immunity on the other hand, the phage DNA accumulated over time to similar levels to those observed in the absence of CRISPR targeting (Figure 3B). Ethidium bromide staining of the digested DNA also revealed a general accumulation of phage DNA (Figure 3C). We corroborated this result using qPCR amplification of the *gp43* target in different infection conditions (Figure 3D). For quantification, the relative abundance of the *gp43* qPCR product detected at 15 min post-infection in cells harboring the *Streptococcus pyogenes* type II-A CRISPR-Cas system was set as the reference point (a value of 1). In these cells, the abundance of the *gp43* qPCR product decreased rapidly with time, showing an efficient destruction of the viral DNA. In cells without CRISPR immunity (carrying a

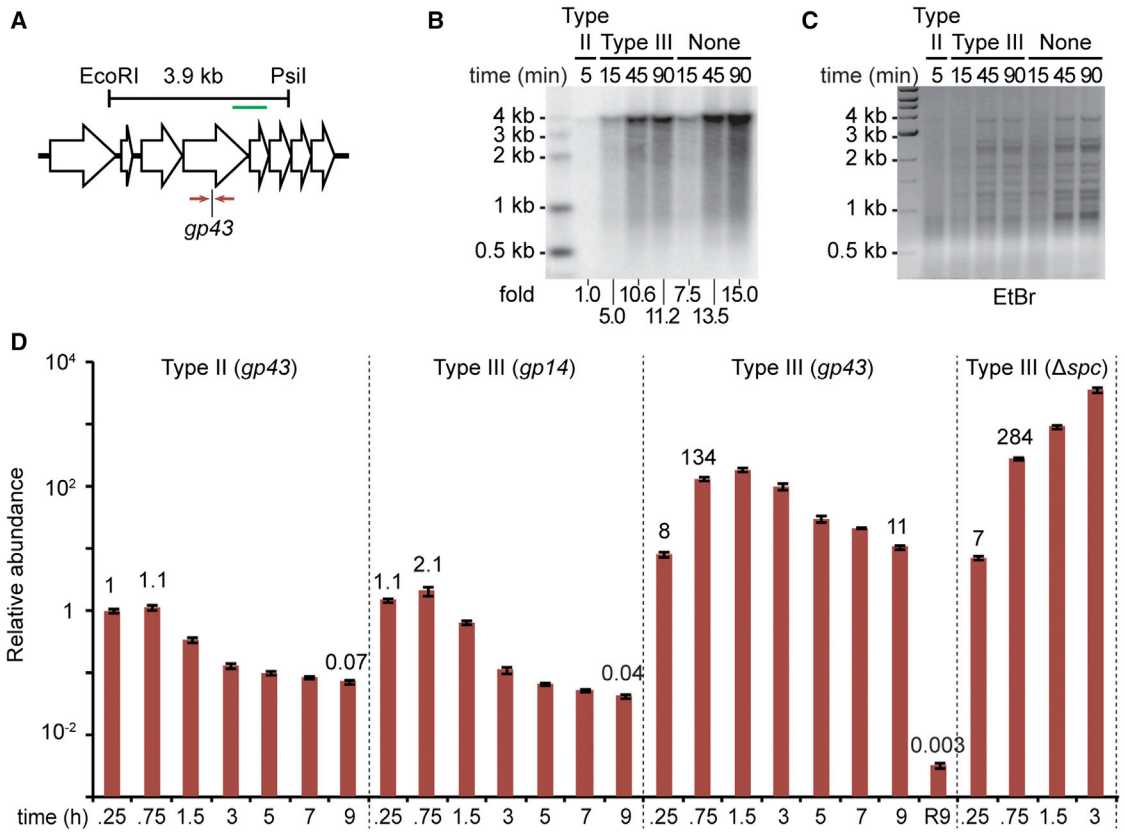

Figure 3. Co-transcriptional Type III CRISPR-Cas Targeting Leads to the Accumulation of Phage DNA

(A) Location of the EcoRI and PsiI restriction sites used to detect phage DNA via southern blot in (B). The green line indicates the location of the dsDNA probe used in this assay. The *gp43* target and the primers (opposed arrows) used for qPCR in (D) are also shown.

(B) Southern blot on total DNA extracted from cells treated with ΦNM1γ6 at different times after infection and digested with EcoRI and PsiI. Cells harboring type II-A or type III-A CRISPR-Cas systems programmed to target the *gp43* gene or without CRISPR-Cas immunity were infected. The intensity, relative to type II-A targeting, of the 3.9-kb phage fragment detected is reported.

(C) Ethidium bromide gel used for southern blot shown in (B).

(D) qPCR performed on the ΦNM1γ6 *gp43* gene using total DNA collected at different times post-infection from cells carrying different CRISPR-Cas systems. Values for the *rho* gene were used for normalization. The normalized value for the measurement at 15 min in cells harboring a type II system was set to 1 to obtain the relative abundance of the *gp43* transcript for the rest of the data points (mean ± SD of four replicas). The R9 time point indicates that cells were refreshed with new culture broth at 9 hr post-infection and were grown for an additional 9 hr before collection of DNA for qPCR.

See also Figure S3.

non-targeting, Δ*spc*, type III-A CRISPR-Cas system), the abundance of the *gp43* qPCR product increased dramatically with time, reflecting the progression of viral replication during the infectious cycle. Phage DNA clearance by type III CRISPR-Cas immunity strongly depended on the region targeted. When the early-expressed gene *gp14* was targeted, the abundance of the *gp43* qPCR product decreased with time similarly to the observations for type II targeting. In contrast, when the late-expressed gene *gp43* was targeted the abundance of the qPCR product reached very high levels before it started a slow decrease. We obtained similar results when we measured phage DNA by qPCR using primers that amplify the *gp14* gene (Figure S3A), showing that DNA abundance at the target as well as at a distant locus is equally affected by CRISPR targeting. Since type III CRISPR-Cas immunity requires transcription across the target for efficient DNA cleavage, we considered the possibility that less transcription across the *gp43* target, compared to transcription of the *gp14* target, could be responsible for the accumulation of phage DNA observed. However, our RNA-seq data indicated that the level of transcription across the *gp14* target at 15 min post-infection is similar or even lower to those of the *gp43* target at 45 min post-infection, when this gene is expressed (cf. 73–130 reads per 500 bases of transcript per million mapped reads [RPM] for *gp14* and *gp43*, respectively; Figures 2D and 2E). Together these results revealed that the requirement of target transcription for type III CRISPR-Cas DNA cleavage results in the accumulation of phage DNA when a region that is expressed late in the infectious cycle is targeted. In vitro, an excess of target DNA prevents efficient cleavage by the Cas10-Csm complex (Figure S3B). We performed a co-transcriptional DNA cleavage assay (Samai et al., 2015) using different complex:target molar ratios, and we found target DNA cleavage at a 10:1, but

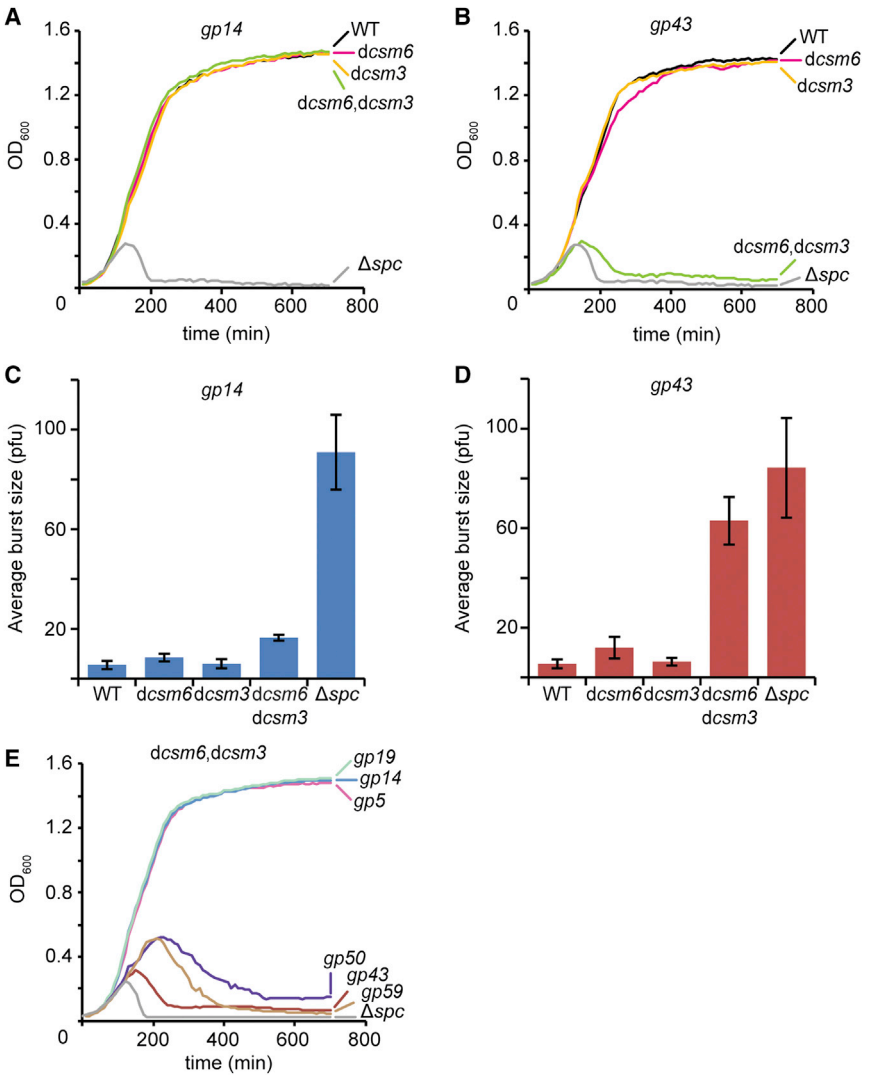

Figure 4. Degradation of Phage Transcripts by Csm3 and Csm6 Enables Type III CRISPR-Cas Immunity Targeting Late-Expressed Genes

(A) Staphylococci harboring different type III-A CRISPR-Cas systems targeting the *gp14* gene were grown in liquid media and infected with ϕNM1γ6 phage (at 0 hr) with a multiplicity of infection of five viruses per bacteria. Optical density at 600 nm (OD_{600}) was measured for the following 12 hr to monitor cell survival due to CRISPR immunity against the phage. Representative growth curves of at least three independent assays are shown.

(B) Same as (A), but with the CRISPR-Cas systems programmed to target *gp43*.

(C) The different infections performed in (A) were plated to enumerate plaque forming units (pfu) and calculate the average burst size. Mean ± SD of three replicas are reported.

(D) Same as (C), but with the CRISPR-Cas systems programmed to target *gp43*.

(E) Survival of cells (determined by measuring growth at OD_{600}) carrying d*csm6*/d*csm3* type III-A CRISPR-Cas systems targeting the different ϕNM1γ6 genes shown in Figure 2A. Representative growth curves of at least three independent assays are shown.

not 1:1, ratio, suggesting that the accumulation of phage DNA observed during the targeting of a late-expressed gene is the result of inefficient DNA cleavage due to the excess of target DNA at this point of the viral infectious cycle. In spite of this significant difference in phage DNA accumulation and cleavage of the target DNA, type III-A CRISPR-Cas systems provide antiviral immunity regardless of the viral genomic region targeted (Goldberg et al., 2014).

Degradation of Phage Transcripts by Csm3 and Csm6 Enables Type III CRISPR-Cas Immunity Targeting Late-Expressed Genes

Previously, we demonstrated that type III-A CRISPR-Cas immunity can protect the host from lysis regardless of the viral genomic region targeted (Goldberg et al., 2014). In light of our results above, we investigated whether the degradation of late-expressed transcripts mediated by Csm3 and Csm6 is also required for CRISPR-Cas immunity during the targeting of late genes. To this end, we compared lysis (measured by absorbance at OD_{600} of the bacterial culture) of infected cells carrying type III-A CRISPR-Cas systems targeting an early- or late-transcribed gene, *gp14* or *gp43*, respectively. The mutants d*csm3*, d*csm6*, and d*csm3*/d*csm6* were as effective as the wild-type CRISPR system to confer immunity via *gp14* targeting (Figure 4A), a result that demonstrates the sufficiency of DNA cleavage for viral clearance in this situation. In contrast, when *gp43* was targeted the d*csm3*/d*csm6* mutant failed to provide immunity (Figure 4B), similarly to a no-targeting control (Δ*spc*). A similar result was obtained when we measured the effect of type III-A CRISPR-Cas immunity on the propagation of the phage by determining the average burst size, i.e., the number of viral particles (counted as plaque forming units, pfu) released per infected cells (Figures 4C and 4D). Both experiments indicate that the RNase activity of either Csm3 or Csm6 is required for immunity when targeting a late-, but not early-, expressed gene. To confirm this pattern, we tested immunity mediated by type III-A d*csm3*/d*csm6* mutant systems targeting two other early-transcribed (*gp5* and *gp19*) and two other late-transcribed (*gp50* and *gp59*) genes (Figure 2A). We infected each strain with ΦNM1γ6 and looked for culture lysis over time (Figure 4E). Whereas targeting of *gp5*, *gp14*, and *gp19* produced efficient immunity, targeting of *gp43*, *gp50*, and *gp59* resulted in the death of bacteria expressing inactive Csm3 and Csm6 RNases. These data demonstrate that the RNase activities of Csm3 and Csm6 are required for type III-A CRISPR-Cas immunity when

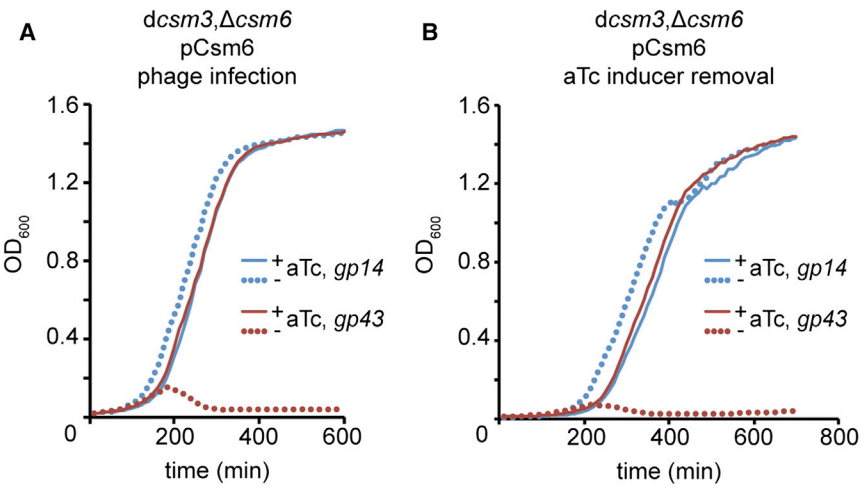

Figure 5. Csm6 Enables Complete Phage Clearance during Immunity against Late-Expressed Genes

(A) Cells harboring Δ*csm6*/d*csm3* type III-A CRISPR-Cas systems targeting *gp14* or *gp43* were complemented with the pCsm6 plasmid, which carries the *csm6* gene under the control of a tetracycline-inducible promoter. Each strain was infected with ϕNM1γ6 in the presence or absence of the aTc (0.008 μg/ml), i.e., induction of Csm6 expression. Bacterial growth was monitored by measuring for OD_{600} for 10 hr.

(B) The cells grown in the presence of aTc were collected, washed to remove the inducer and eliminate further expression of Csm6, and diluted (1:333) in fresh media without phage nor aTc. As a control an aliquot of the washed cells were re-inoculated in fresh media with aTc (0.008 μg/ml). Bacterial growth was monitored by measuring for OD_{600} for 12 hr.

the targets specified by the crRNA guide reside within late-expressed genes.

We showed that the accumulation of phage DNA that occurs prior to the targeting of late-expressed genes prevents the type III-A CRISPR-Cas system from rapidly clearing the phage DNA. In this scenario, we hypothesized that the degradation of phage transcripts by Csm3 and Csm6 limits further viral gene expression and the continuation of the lytic infectious cycle, which would otherwise compromise host cell viability. To test this, we designed an experiment to eliminate RNase activity 10 hr post-infection. We infected cells harboring d*csm3*/Δ*csm6* CRISPR-Cas systems targeting *gp14* or *gp43* and carrying the pCsm6 plasmid, which provides aTc-dependent expression of Csm6 (Figure 5A). As expected from our previous results, in the absence of the inducer the cells targeting *gp43*, but not those targeting *gp14*, succumbed to phage infection. In the presence of aTc, both populations survived. The cells from these two populations were washed with fresh broth to eliminate aTc, and thus Csm6 expression, 10 hr after the addition of ΦNM1γ6 to the cultures. Cells were diluted in fresh broth with or without aTc, and their growth was monitored by following absorbance at OD_{600} (Figure 5B). While the growth of *gp14*-targeting cells was not affected by removal of Csm6, *gp43*-targeting cells were lysed by phage. This result demonstrates that without the degradation of phage transcripts by Csm6, the phage lytic cycle can continue in spite of DNA cleavage, leading to the death of the host cells.

Csm6 Is Required to Provide Immunity against Viruses with Target Mutations

Our data show that the targeting of a late-expressed gene leads to the accumulation of target DNA and that in this scenario the RNase activities of Csm3 or Csm6 are required to clear the phage transcripts and slow down the phage lytic cycle until all DNA targets are destroyed. A similar situation could present during infection with phages harboring target mismatches. In both type I and type II CRISPR-Cas immunity, mutations in the target region lead to the escape of mutant phages due to a reduced crRNA-guided DNA cleavage. Type III CRISPR-Cas systems, however, seem much more tolerant of such mutations and are able to provide immunity even in the presence of several mismatches within the crRNA:target interaction (Goldberg et al., 2014; Manica et al., 2013). We speculated that, if target mutations result in inefficient DNA cleavage also during type III CRISPR-Cas immunity, the reported tolerance to mutations could be the result of phage transcript cleavage by the Csm3 and/or Csm6 RNase activity. To test this, we introduced three, four, and five mismatches into the spacer sequence targeting the *gp43* gene of ΦNM1γ6 (Figure 6A). We infected hosts carrying these mutations and looked for the CRISPR immune response (Figure 6B). Consistent with previous reports, type III CRISPR-Cas immunity protected staphylococci even in the presence of three and four mismatches (but not five) between the crRNA guide and its target. We first tested whether Csm6 was important for immunity in the presence of mismatches by performing infections in a Δ*csm6* host (Figure 6C). Consistent with Figure 4B, *csm6* was not required to provide immunity when the phage carried a target with perfect homology. However, cells were not as protected in the presence of three mismatches, and immunity was completely abrogated with four mismatches in the crRNA:target interaction. Protection in the presence of four mismatches required the RNase activity of Csm6 (Figure S4A). In contrast, the RNase activity of Csm3 was not required for immunity in the presence of four mismatches (Figure S4A). We used qPCR of the *gp43* target to compare phage DNA accumulation during the course of infection of wild-type hosts carrying a perfectly matching or four-mismatch spacer (Figure 6D). We observed that indeed the presence of mismatches led to the accumulation of target phage DNA. This was corroborated by an anti-plasmid immunity assay similar to the one presented in Figure 1D using a four-mismatch target (Figures 6E and S4B).

Target mismatches are not only present within a viral population but are very common between related phages. For example, we previously engineered a spacer matching the *gp32* gene present in the staphylococcal phage ΦNM1γ6 (Goldberg et al., 2014), which has four mismatches to the same gene in the related phage ΦNM4γ4 (Bae et al., 2006; Heler et al., 2015) (Figure 6F). Consistent with our results, type III-A CRISPR-Cas

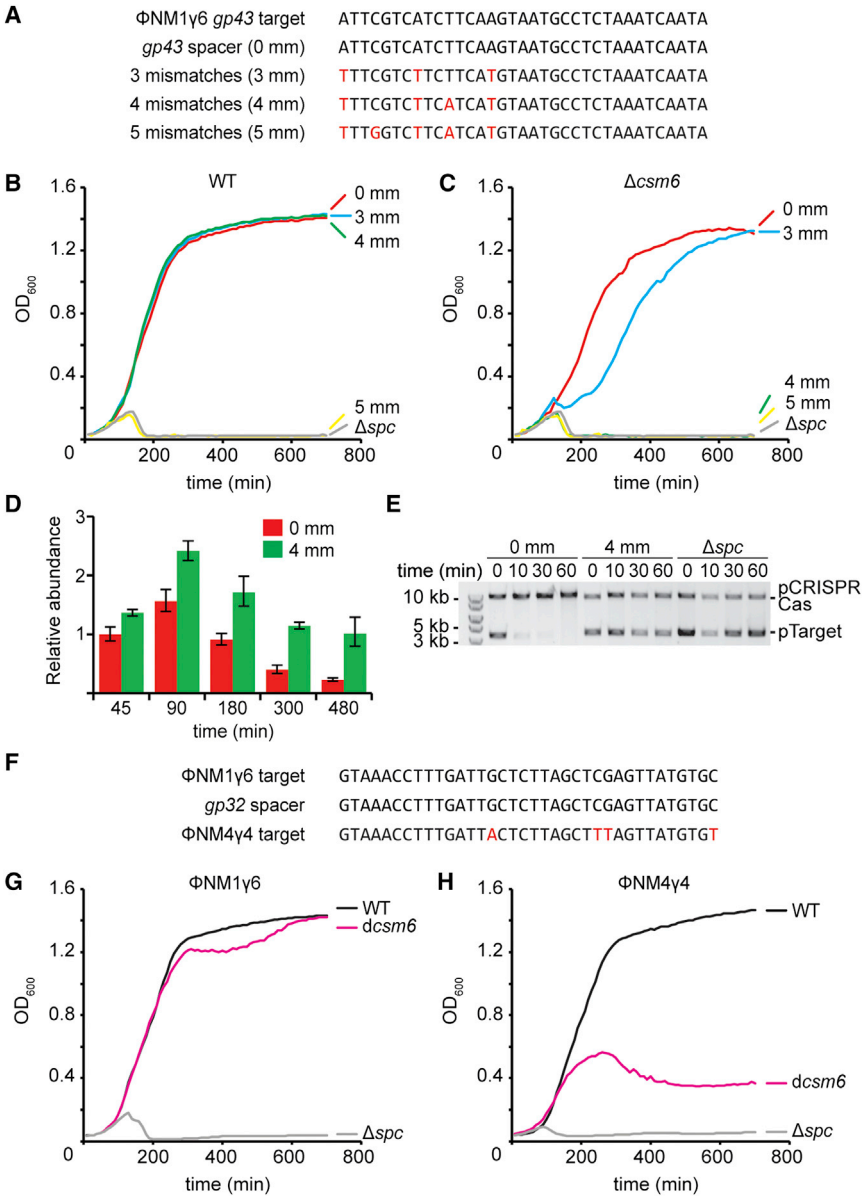

Figure 6. Csm6 Is Required to Provide Immunity against Viruses with Target Mutations

(A) Introduction of mutations (in red) in the spacer targeting the *gp43* phage gene that generate three, four, or five mismatches in the crRNA:target region.

(B) Staphylococci harboring a wild-type III-A CRISPR-Cas system targeting the *gp43* gene in the presence of different crRNA:target mismatches were grown in liquid media and infected with ϕNM1γ6 phage (at 0 hr) with a multiplicity of infection of five viruses per bacteria. Optical density at 600 nm (OD_{600}) was measured for the following 12 hr to monitor cell survival. Representative growth curves of at least three independent assays are shown.

(C) Same as (B), but with cells harboring a CRISPR-Cas locus without *csm6*.

(D) qPCR performed on the ΦNM1γ6 *gp43* gene using total DNA collected at different times post-infection from cells carrying CRISPR-Cas systems targeting in the presence (4 mm) or absence (0 mm) of crRNA:target mismatches. Values for the *rho* gene were used for normalization to obtain the relative abundance of the *gp43* gene for each data point (mean ± SD of four replicas).

(E) pTarget plasmid DNA, harboring the *gp43* target under the control of a tetracycline-inducible promoter, was extracted from cells harboring a type III-A CRISPR-Cas system without a spacer (Δ*spc*) or with a gp43-targeting spacer with or without mismatches (4 or 0 mm, respectively), at different times after treatment with aTc. Plasmid DNA was visualized by agarose gel electrophoresis followed by ethidium bromide staining.

(F) The *gp32* spacer has a complete match in the ϕNM1γ6 genome but presents four mismatches in the ϕNM4γ4 phage.

(G) Staphylococci harboring a wild-type, Δ*csm6*, or Δ*spc* type III-A CRISPR-Cas system with the *gp32* spacer were grown in liquid media and infected with ϕNM1γ6 phage (at 0 hr) with a multiplicity of infection of five viruses per bacteria. Optical density at 600 nm (OD_{600}) was measured for the following 12 hr to monitor cell survival due to CRISPR immunity against the phage. Representative growth curves of at least three independent assays are shown.

(H) Same as (G), but following infection with phage ϕNM4γ4.

See also Figure S4.

immunity against ΦNM1γ6 mediated by this spacer does not require the RNase activity of Csm6 (Figure 6G). In contrast, whereas the wild-type CRISPR-Cas system tolerated the four mismatches and protected cells from ΦNM4γ4 infection, the d*csm6* mutant cells were susceptible to viral attack (Figure 6H). Together these results show that Csm6 RNase activity is required to maintain immunity in the presence of target mutations that decrease the efficiency of DNA targeting, a distinct property of type III systems.

DISCUSSION

Type III CRISPR-Cas systems cleave both the genome and the transcripts of invaders (Peng et al., 2015; Samai et al., 2015). Whereas DNA cleavage is fundamental for CRISPR immunity against these invaders, a role for the RNase activity of these systems has been elusive. A recent report showed that the Cas10-Csm complex could prevent the propagation of ssRNA phages in *E. coli* (Tamulaitis et al., 2014). However, these types of viruses are rare in the prokaryotic world (Koonin et al., 2015), and CRISPR spacer sequences that match RNA viruses have not yet been found. In addition, it has been argued that due to the high mutation rate of RNA viruses (about three orders of magnitude above that of dsDNA viruses), maintaining long-term immunity against these invaders would require an extremely rapid acquisition of new spacer sequences (Weinberger and Gilmore, 2015; Weinberger et al., 2012). Therefore, a role for type III CRISPR-Cas system providing immunity against RNA viruses

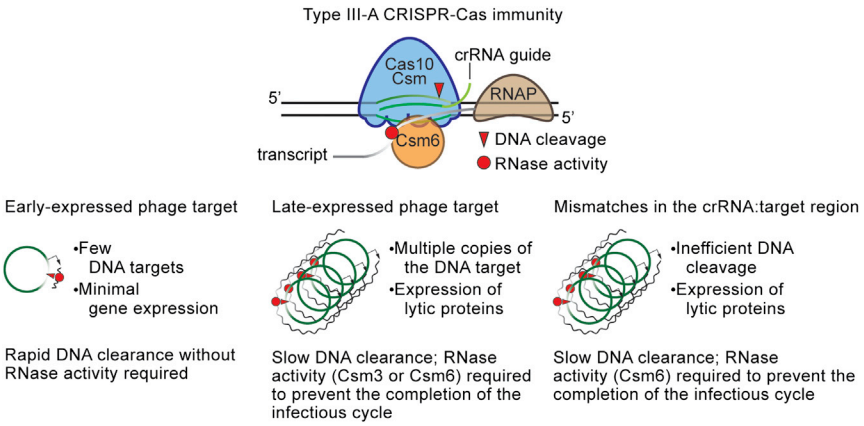

Figure 7. A Model for the Requirement for Transcript Degradation during Type III CRISPR-Cas Immunity

The type III-A Cas10-Csm complex performs co-transcriptional cleavage of the target DNA and its transcripts. Within this complex, Cas10 contains the DNase activity and Csm3 is an RNase. Csm6 is another type III-A RNase that degrades target transcripts. This molecular mechanism of immunity allows for the rapid attack of the viral genome when early-expressed targets are specified by the crRNA guide, which leads to fast and efficient degradation of the invader's genetic material and the clearance of the infection without the need of RNase activity. In contrast, the targeting of a late-expressed gene allows viral replication and transcription before DNA cleavage can occur. The accumulated genomes are not cleared efficiently by the endonuclease activity of the Cas10 complex, and the degradation of phage transcripts by Csm3 or Csm6 is required to prevent the completion of the infectious cycle and the lysis of the host cell. Similarly, the presence of crRNA:target mismatches within the phage population prevents efficient DNA cleavage that also leads to the accumulation of phage genomes in the cell. In this scenario, the Csm6 RNase is required for transcript degradation and survival.

in a natural setting remains to be determined. Here, we showed a role for transcript degradation in the immunity mechanism against dsDNA phages, predicted to be the most common type of viruses that infect prokaryotes (Koonin et al., 2015), provided by the type III-A CRISPR-Cas system of *S. epidermidis*. We found that these systems encode two RNases, Csm3, and Csm6, that are required to provide immunity against dsDNA phages when the crRNA guide of the Cas10-Csm complex matches late-, but not early-, expressed genes. We propose that as a consequence of the co-transcriptional DNA cleavage activity of type III CRISPR-Cas systems, which cannot cleave the viral DNA until the target is transcribed, the targeting of late phage genes results in the accumulation of viral genomes. In this scenario, the RNase activities of the type III-A CRISPR-Cas system are required to degrade phage transcripts and prevent the completion of the viral infectious cycle until all the viral genomes are cleared (Figure 7). In contrast, when an early-transcribed gene is targeted, DNA cleavage occurs shortly after genome injection. In this case, the endonuclease activity of the Cas10-Csm complex is sufficient to clear the virus; the infectious cycle does not proceed further and the degradation of phage transcripts is not necessary to prevent phage propagation.

All the staphylococcal phages characterized so far belong to the *Caudovirales* order and are mainly temperate *Siphoviridae* (Deghorain and Van Melderen, 2012), such as ΦNM1. A small number belong to the *Podoviridae* or *Myoviridae* family. Regardless of the different genomic organizations and infectious cycles, all of these phages present a tight regulation of gene expression (Kwan et al., 2005), and therefore different sets of genes are transcribed at different times post-infection. We believe that the ability of transcript degradation by type III-A CRISPR-Cas systems would be important to provide immunity against most classes of dsDNA viruses when the crRNA guide targets genes that are expressed late in the infectious cycle. Target selection occurs during the "adaptation" phase of CRISPR-Cas immunity, when new spacer sequences from an invading phage are incorporated into the CRISPR array (Heler et al., 2014). Although little is known about the acquisition of spacers by type III CRISPR-Cas systems, type I and II systems incorporate spacers matching all regions of the viral genome (Datsenko et al., 2012; Heler et al., 2015; Paez-Espino et al., 2013), without any noticeable bias toward early or late genes. If such bias is also absent during spacer acquisition by type III CRISPR-Cas systems, the RNase activity would be necessary to confer immunity to all bacteria that incorporate a spacer specifying a late-expressed gene.

Our studies showed that either Csm3 or Csm6 RNase activity is required for immunity when the target of the Cas10-Csm complex is located in a late-expressed gene. Mutations in the active sites of either of these genes are not sufficient to disrupt immunity. However, in the presence of target mismatches that lead to the accumulation of phage DNA, the RNase activity of Csm6, but not that of Csm3, is required for immunity. This is an important function that distinguishes the type III from the type I and II CRISPR immune response. Whereas type I and II CRISPR immunity is very sensitive to mutations in the target sequence (especially in the "seed" region of the target) (Gasiunas et al., 2012; Jinek et al., 2012; Westra et al., 2012; Wiedenheft et al., 2011), type III immunity is unusually tolerant of such mutations (Goldberg et al., 2014; Manica et al., 2013), allowing the targeting of "escape" or related viruses. In all three systems, target mutations prevent efficient DNA cleavage; however, in type III systems, transcript degradation by Csm6 results in robust immunity, presumably by stalling the progression of the phage lytic cycle and allowing for more time for phage DNA clearance (Figure 7). Here, we found that the most dramatic results were obtained in the presence of four mismatches, but we suspect that this number may vary for different target sequences. Mismatches may not be the only condition in which one or the other RNase activity of type III systems is required. We speculate that in other scenarios that lead to the accumulation of phage DNA in the cell, such as infection by phages with particular propagation cycles, by phages that introduce modifications to their nucleic acids, or in selected habitats (type III systems are predominant in thermophilic archaea; Makarova et al., 2011a), one or the other

RNase activity may be more important to allow for complete DNA clearance.

Whereas Csm3 is part of the Cas10-Csm complex and cleaves sequences that are specified by the crRNA guide (Samai et al., 2015; Staals et al., 2014; Tamulaitis et al., 2014), Csm6 is not part of the complex and has crRNA-independent activity. Although these mechanisms of RNA cleavage are considerably different, both are sufficient to degrade phage transcripts and facilitate type III-A CRISPR-Cas immunity in the conditions tested in this study. How Csm6 achieves specificity for phage transcripts is not known. One possible mechanism to restrict Csm6 activity to the Cas10-Csm target would be the existence of a biophysical interaction between them during targeting. Additional work focused on Csm6 will address its specificity and its role during plasmid conjugation, two intriguing properties of this RNase.

While Csm6 is associated with type III-A CRISPR-Cas systems, some type III-B systems harbor a Csm6 ortholog, Csx1 (Makarova et al., 2011a, 2011b, 2015), which also belongs to the HEPN family (Anantharaman et al., 2013). Based on our results obtained for Csm6 and the sequence similarity between these genes, we propose that Csx1 also provides crRNA-independent RNase activity to the type III-B CRISPR-Cas systems. Our work also predicts that Csx1 and the Cmr4 crRNA-guided RNA nuclease (the Csm3 ortholog) within the Cas10-Cmr complex (Benda et al., 2014; Hale et al., 2014; Ramia et al., 2014) may be required for the targeting of late-expressed genes in dsDNA phages by these systems. Future experiments will consider this and other intriguing aspects of these elaborate immune systems.

EXPERIMENTAL PROCEDURES

Bacterial Strains and Growth Conditions

Cultivation of *E. coli* was done in Luria-Bertani (LB) medium (BD Biosciences) or Terrific Broth medium (Fisher Scientific) at 37°C. Whenever applicable, media were supplemented with 100 μg/ml ampicilin or 34 μg/ml chloramphenicol to ensure plasmid maintenance.

All in vivo experiments were performed in *S. aureus* RN4220 (Kreiswirth et al., 1983). Cultivation of *S. aureus* RN4220 was done in tryptic soy broth (TSB) medium (BD Biosciences) at 37°C. Whenever applicable, media were supplemented with chloramphenicol or erythromycin at 10 μg/ml to ensure plasmid maintenance. When appropriate, anhydrotetracycline (aTc) was used at a concentration of 0.25 μg/ml (unless otherwise indicated) to initiate transcription from the P_{tet} promoter.

Plasmid Cloning

See Supplemental Experimental Procedures.

Plasmid DNA Preparation

Plasmid DNA was purified from 2–6 ml of *E. coli* DH5α or *S. aureus* RN4220 overnight cultures. For preparation from *S. aureus* cultures, cells were pelleted, re-suspended in 100 μl Tris-sucrose-magnesium buffer (TSM) buffer (50 mM Tris-HCl [pH 7.5], 10 mM $MgCl_2$, 0.5 M sucrose), and then treated with 5 μl lysostaphin (2 mg ml^{-1}) at 37°C for 1 hr before treatment with plasmid miniprep reagents from QIAGEN. Purification used QIAGEN or EconoSpin columns.

Purification of Csm6

Purification was performed via Ni-NTA affinity chromatography. See Supplemental Experimental Procedures for details.

Csm6 RNA Cleavage Assay

RNA cleavage reactions were performed at 37°C with 1 μM of 5′-radiolabeled (R55 and R24) and 3′-radiolabeled ssRNA (R55) substrates and 10 μM of wild-type or mutant Csm6. The reaction was carried out in reaction buffer containing 50 mM Tris-HCl (pH 7.5), 30 mM NaCl, 2 mM DTT, and 1% glycerol. Reaction mixtures were withdrawn at specified time intervals and subsequently quenched with 90% formamide and 50 mM EDTA. Reaction products were separated by denaturing PAGE, and the gel was visualized by phosphorimaging. The 5′-radiolabeled decade RNA ladder (Life Technologies) was used as a size marker.

Csm6 DNA Cleavage Assay

DNA cleavage reactions were performed at 37°C for up to 2 hr with 1 μM of 5′-radiolabeled ssDNA (PS362) and dsDNA (PS362/PS363) substrates and 10 μM of wild-type Csm6. The reaction was carried out in reaction buffer containing 50 mM Tris-HCl (pH 7.5), 10 mM $MgCl_2$, 30 mM NaCl, 2 mM DTT, and 1% glycerol. Reaction mixtures were withdrawn at specified time intervals and subsequently quenched with 90% formamide and 50 mM EDTA. Reaction products were separated by denaturing PAGE, and the gel was visualized by phosphorimaging. The 5′-radiolabeled 10-bp DNA ladder (Promega) was used as a size marker.

Transcription Coupled DNA Cleavage

Transcription coupled DNA cleavage were performed as previously described (Samai et al., 2015). See Supplemental Experimental Procedures for details.

Preparation of Electrocompetent *S. aureus* Cells

Preparation of *S. aureus* RN4220 competent cells and DNA transformation was performed as previously described (Goldberg et al., 2014).

Phage Infections and Plate Reader Growth Curves

Infection of *S. aureus* RN4220 cells with bacteriophage ΦNM1γ6 or ΦNM4γ4 was performed as described previously (Goldberg et al., 2014). See Supplemental Experimental Procedures for details.

Measurement of Average Burst Size

RN4220 cells with appropriate CRISPR-Cas plasmids were grown in TSB supplemented with 5 mM $CaCl_2$ and appropriate antibiotics to an OD_{600} of 0.3–0.5. Cells were infected by ΦNM1γ6 at MOI = 0.1 for 5 min. Cells were immediately washed in TSB twice at 4°C and re-suspended in equal initial volume. An aliquot of cells were spotted on heart infusion (BD Biosciences) soft agar plates with a sensitive lawn (i.e., RN4220). The rest of the cells were incubated at 37°C for another 75 min before an aliquot of cells were spotted on a sensitive lawn. Agar plates were incubated at 37°C for 16–20 hr before plaques were enumerated. Average burst size was calculated as the ratio of plaques formed at 80 min to plaques formed at 5 min for each strain of interest.

Total RNA Extraction

Total RNA extraction was performed as previously described (Samai et al., 2015). See Supplemental Experimental Procedures for details.

Total DNA Extraction

Total DNA extraction was performed as previously described (Samai et al., 2015). See Supplemental Experimental Procedures for details.

Plasmid-Curing Assay

Plasmid-curing assay was performed as previously described (Samai et al., 2015). See Supplemental Experimental Procedures for details.

Primer Extension

Primer extension assays were performed as previously described (Hatoum-Aslan et al., 2011) using primer A248.

qPCR

Cells were infected by ΦNM1γ6 (MOI = 5) during early log phase (at OD_{600} of 0.3–0.4). qPCR was performed using Fast SYBR Green Master Mix (Life Technologies) and 7900HT Fast Real-Time PCR System (Applied Biosystems). For

RNA samples, total RNA was treated with DNase I (Sigma-Aldrich). 1 μg of DNase-I-treated RNA samples was subjected to RT using M-MuLV Reverse Transcriptase (NEB) and 100 ng of random hexamer (Invitrogen) according to the NEB protocol. The resulting cDNA was diluted five times as stocks. 500 nM of primers was used and 0.2 μl of the cDNA stock was used as template for a 10-μl reaction according to the Fast SYBR Green Master Mix protocol. For DNA samples, 25 ng of total DNA was used as template. The housekeeping *rho* gene was used as endogenous control for normalization (Theis et al., 2007). Primers used for amplification are shown in Table S2.

RNA Sequencing

Total RNA was treated with DNase I (Sigma-Aldrich) and subjected to TruSeq Stranded mRNA Library Prep Kit (Illumina) without rRNA depletion and Illumina NextSeq. Reads were aligned to reference genomes using Bowtie and sorted using SAMtools. Using a custom script, sorted reads were accessed via Pysam, normalized as reads per million values, and plotted as the average over consecutive windows of 500 bp using matplotlib tools for IPython.

Southern Blot

20 μg of total DNA prepared from infected cells were digested with restriction enzymes EcoRI and PsiI for 5 hr and resolved on a 1% argarose gel. DNA fragments were transferred from the gel via capillary action to a Hybond membrane (GE Healthcare) using alkaline transfer (Sambrook et al., 1989). Probes were produced via PCR of ΦNM1γ6 DNA using primers W865/W866, and α-^{32}P-dATP in addition to regular dNTPs. Hybridization was performed at 65°C overnight in Church buffer (Sambrook et al., 1989).

SUPPLEMENTAL INFORMATION

Supplemental Information includes Supplemental Experimental Procedures, four figures, and three tables and can be found with this article online at http://dx.doi.org/10.1016/j.cell.2015.12.053.

AUTHOR CONTRIBUTIONS

W.J. performed all the experiments in this paper. P.S. purified wild-type and mutant versions of Csm6 and performed biochemical assays. L.A.M. and W.J. wrote the manuscript.

ACKNOWLEDGMENTS

We would like to thank Andrew Varble, Gregory Goldberg, and Nora Pyenson for critical reading of the manuscript. We are grateful to Gregory Goldberg for initial demonstrations of the *csm6*-independent chromosomal targeting. We thank the Rockefeller University Genomics Resource Center for performing the RNA-seq experiments. We are grateful to the Tavazoie lab for help with qRT-PCR. P.S. is supported by a Helmsley Postdoctoral Fellowship for Basic and Translational Research on Disorders of the Digestive System at The Rockefeller University. L.A.M. is supported by the Rita Allen Scholars Program, an Irma T. Hirschl Award, a Sinsheimer Foundation Award and a NIH Director's New Innovator Award (1DP2AI104556-01).

Received: July 10, 2015
Revised: October 30, 2015
Accepted: December 21, 2015
Published: February 4, 2016

REFERENCES

Anantharaman, V., Makarova, K.S., Burroughs, A.M., Koonin, E.V., and Aravind, L. (2013). Comprehensive analysis of the HEPN superfamily: identification of novel roles in intra-genomic conflicts, defense, pathogenesis and RNA processing. Biol. Direct *8*, 15.

Arslan, Z., Hermanns, V., Wurm, R., Wagner, R., and Pul, Ü. (2014). Detection and characterization of spacer integration intermediates in type I-E CRISPR-Cas system. Nucleic Acids Res. *42*, 7884–7893.

Bae, T., Baba, T., Hiramatsu, K., and Schneewind, O. (2006). Prophages of *Staphylococcus aureus* Newman and their contribution to virulence. Mol. Microbiol. *62*, 1035–1047.

Barrangou, R., Fremaux, C., Deveau, H., Richards, M., Boyaval, P., Moineau, S., Romero, D.A., and Horvath, P. (2007). CRISPR provides acquired resistance against viruses in prokaryotes. Science *315*, 1709–1712.

Benda, C., Ebert, J., Scheltema, R.A., Schiller, H.B., Baumgärtner, M., Bonneau, F., Mann, M., and Conti, E. (2014). Structural model of a CRISPR RNA-silencing complex reveals the RNA-target cleavage activity in Cmr4. Mol. Cell *56*, 43–54.

Bolotin, A., Quinquis, B., Sorokin, A., and Ehrlich, S.D. (2005). Clustered regularly interspaced short palindrome repeats (CRISPRs) have spacers of extrachromosomal origin. Microbiology *151*, 2551–2561.

Brouns, S.J., Jore, M.M., Lundgren, M., Westra, E.R., Slijkhuis, R.J., Snijders, A.P., Dickman, M.J., Makarova, K.S., Koonin, E.V., and van der Oost, J. (2008). Small CRISPR RNAs guide antiviral defense in prokaryotes. Science *321*, 960–964.

Carte, J., Wang, R., Li, H., Terns, R.M., and Terns, M.P. (2008). Cas6 is an endoribonuclease that generates guide RNAs for invader defense in prokaryotes. Genes Dev. *22*, 3489–3496.

Datsenko, K.A., Pougach, K., Tikhonov, A., Wanner, B.L., Severinov, K., and Semenova, E. (2012). Molecular memory of prior infections activates the CRISPR/Cas adaptive bacterial immunity system. Nat. Commun. *3*, 945.

Deghorain, M., and Van Melderen, L. (2012). The Staphylococci phages family: an overview. Viruses *4*, 3316–3335.

Deltcheva, E., Chylinski, K., Sharma, C.M., Gonzales, K., Chao, Y., Pirzada, Z.A., Eckert, M.R., Vogel, J., and Charpentier, E. (2011). CRISPR RNA maturation by trans-encoded small RNA and host factor RNase III. Nature *471*, 602–607.

Deng, L., Garrett, R.A., Shah, S.A., Peng, X., and She, Q. (2013). A novel interference mechanism by a type IIIB CRISPR-Cmr module in *Sulfolobus*. Mol. Microbiol. *87*, 1088–1099.

Garneau, J.E., Dupuis, M.E., Villion, M., Romero, D.A., Barrangou, R., Boyaval, P., Fremaux, C., Horvath, P., Magadán, A.H., and Moineau, S. (2010). The CRISPR/Cas bacterial immune system cleaves bacteriophage and plasmid DNA. Nature *468*, 67–71.

Gasiunas, G., Barrangou, R., Horvath, P., and Siksnys, V. (2012). Cas9-crRNA ribonucleoprotein complex mediates specific DNA cleavage for adaptive immunity in bacteria. Proc. Natl. Acad. Sci. USA *109*, E2579–E2586.

Goldberg, G.W., Jiang, W., Bikard, D., and Marraffini, L.A. (2014). Conditional tolerance of temperate phages via transcription-dependent CRISPR-Cas targeting. Nature *514*, 633–637.

Hale, C.R., Zhao, P., Olson, S., Duff, M.O., Graveley, B.R., Wells, L., Terns, R.M., and Terns, M.P. (2009). RNA-guided RNA cleavage by a CRISPR RNA-Cas protein complex. Cell *139*, 945–956.

Hale, C.R., Cocozaki, A., Li, H., Terns, R.M., and Terns, M.P. (2014). Target RNA capture and cleavage by the Cmr type III-B CRISPR-Cas effector complex. Genes Dev. *28*, 2432–2443.

Hatoum-Aslan, A., Maniv, I., and Marraffini, L.A. (2011). Mature clustered, regularly interspaced, short palindromic repeats RNA (crRNA) length is measured by a ruler mechanism anchored at the precursor processing site. Proc. Natl. Acad. Sci. USA *108*, 21218–21222.

Hatoum-Aslan, A., Samai, P., Maniv, I., Jiang, W., and Marraffini, L.A. (2013). A ruler protein in a complex for antiviral defense determines the length of small interfering CRISPR RNAs. J. Biol. Chem. *288*, 27888–27897.

Hatoum-Aslan, A., Maniv, I., Samai, P., and Marraffini, L.A. (2014). Genetic characterization of antiplasmid immunity through a type III-A CRISPR-Cas system. J. Bacteriol. *196*, 310–317.

Heler, R., Marraffini, L.A., and Bikard, D. (2014). Adapting to new threats: the generation of memory by CRISPR-Cas immune systems. Mol. Microbiol. *93*, 1–9.

Heler, R., Samai, P., Modell, J.W., Weiner, C., Goldberg, G.W., Bikard, D., and Marraffini, L.A. (2015). Cas9 specifies functional viral targets during CRISPR-Cas adaptation. Nature *519*, 199–202.

Jinek, M., Chylinski, K., Fonfara, I., Hauer, M., Doudna, J.A., and Charpentier, E. (2012). A programmable dual-RNA-guided DNA endonuclease in adaptive bacterial immunity. Science *337*, 816–821.

Koonin, E.V., Krupovic, M., and Yutin, N. (2015). Evolution of double-stranded DNA viruses of eukaryotes: from bacteriophages to transposons to giant viruses. Ann. N Y Acad. Sci. *1341*, 10–24.

Kreiswirth, B.N., Löfdahl, S., Betley, M.J., O'Reilly, M., Schlievert, P.M., Bergdoll, M.S., and Novick, R.P. (1983). The toxic shock syndrome exotoxin structural gene is not detectably transmitted by a prophage. Nature *305*, 709–712.

Kwan, T., Liu, J., DuBow, M., Gros, P., and Pelletier, J. (2005). The complete genomes and proteomes of 27 Staphylococcus aureus bacteriophages. Proc. Natl. Acad. Sci. USA *102*, 5174–5179.

Makarova, K.S., Aravind, L., Wolf, Y.I., and Koonin, E.V. (2011a). Unification of Cas protein families and a simple scenario for the origin and evolution of CRISPR-Cas systems. Biol. Direct *6*, 38.

Makarova, K.S., Haft, D.H., Barrangou, R., Brouns, S.J., Charpentier, E., Horvath, P., Moineau, S., Mojica, F.J., Wolf, Y.I., Yakunin, A.F., et al. (2011b). Evolution and classification of the CRISPR-Cas systems. Nat. Rev. Microbiol. *9*, 467–477.

Makarova, K.S., Wolf, Y.I., Alkhnbashi, O.S., Costa, F., Shah, S.A., Saunders, S.J., Barrangou, R., Brouns, S.J., Charpentier, E., Haft, D.H., et al. (2015). An updated evolutionary classification of CRISPR-Cas systems. Nat. Rev. Microbiol. *13*, 722–736.

Manica, A., Zebec, Z., Steinkellner, J., and Schleper, C. (2013). Unexpectedly broad target recognition of the CRISPR-mediated virus defence system in the archaeon *Sulfolobus solfataricus*. Nucleic Acids Res. *41*, 10509–10517.

Marraffini, L.A., and Sontheimer, E.J. (2008). CRISPR interference limits horizontal gene transfer in staphylococci by targeting DNA. Science *322*, 1843–1845.

Mojica, F.J., Díez-Villaseñor, C., García-Martínez, J., and Soria, E. (2005). Intervening sequences of regularly spaced prokaryotic repeats derive from foreign genetic elements. J. Mol. Evol. *60*, 174–182.

Nuñez, J.K., Kranzusch, P.J., Noeske, J., Wright, A.V., Davies, C.W., and Doudna, J.A. (2014). Cas1-Cas2 complex formation mediates spacer acquisition during CRISPR-Cas adaptive immunity. Nat. Struct. Mol. Biol. *21*, 528–534.

Nuñez, J.K., Lee, A.S., Engelman, A., and Doudna, J.A. (2015). Integrase-mediated spacer acquisition during CRISPR-Cas adaptive immunity. Nature *519*, 193–198.

Paez-Espino, D., Morovic, W., Sun, C.L., Thomas, B.C., Ueda, K., Stahl, B., Barrangou, R., and Banfield, J.F. (2013). Strong bias in the bacterial CRISPR elements that confer immunity to phage. Nat. Commun. *4*, 1430.

Peng, W., Feng, M., Feng, X., Liang, Y.X., and She, Q. (2015). An archaeal CRISPR type III-B system exhibiting distinctive RNA targeting features and mediating dual RNA and DNA interference. Nucleic Acids Res. *43*, 406–417.

Pourcel, C., Salvignol, G., and Vergnaud, G. (2005). CRISPR elements in *Yersinia pestis* acquire new repeats by preferential uptake of bacteriophage DNA, and provide additional tools for evolutionary studies. Microbiology *151*, 653–663.

Ramia, N.F., Spilman, M., Tang, L., Shao, Y., Elmore, J., Hale, C., Cocozaki, A., Bhattacharya, N., Terns, R.M., Terns, M.P., et al. (2014). Essential structural and functional roles of the Cmr4 subunit in RNA cleavage by the Cmr CRISPR-Cas complex. Cell Rep. *9*, 1610–1617.

Samai, P., Pyenson, N., Jiang, W., Goldberg, G.W., Hatoum-Aslan, A., and Marraffini, L.A. (2015). Co-transcriptional DNA and RNA cleavage during type III CRISPR-Cas immunity. Cell *161*, 1164–1174.

Sambrook, J., Fritsch, E.F., and Maniatis, T. (1989). Molecular Cloning: A Laboratory Manual (Cold Spring Harbor Laboratory Press).

Staals, R.H., Zhu, Y., Taylor, D.W., Kornfeld, J.E., Sharma, K., Barendregt, A., Koehorst, J.J., Vlot, M., Neupane, N., Varossieau, K., et al. (2014). RNA targeting by the type III-A CRISPR-Cas Csm complex of *Thermus thermophilus*. Mol. Cell *56*, 518–530.

Tamulaitis, G., Kazlauskiene, M., Manakova, E., Venclovas, Č., Nwokeoji, A.O., Dickman, M.J., Horvath, P., and Siksnys, V. (2014). Programmable RNA shredding by the type III-A CRISPR-Cas system of *Streptococcus thermophilus*. Mol. Cell *56*, 506–517.

Theis, T., Skurray, R.A., and Brown, M.H. (2007). Identification of suitable internal controls to study expression of a Staphylococcus aureus multidrug resistance system by quantitative real-time PCR. J. Microbiol. Methods *70*, 355–362.

Weinberger, A.D., and Gilmore, M.S. (2015). A CRISPR View of Cleavage. Cell *161*, 964–966.

Weinberger, A.D., Wolf, Y.I., Lobkovsky, A.E., Gilmore, M.S., and Koonin, E.V. (2012). Viral diversity threshold for adaptive immunity in prokaryotes. MBio *3*, e00456-12.

Westra, E.R., van Erp, P.B., Künne, T., Wong, S.P., Staals, R.H., Seegers, C.L., Bollen, S., Jore, M.M., Semenova, E., Severinov, K., et al. (2012). CRISPR immunity relies on the consecutive binding and degradation of negatively supercoiled invader DNA by Cascade and Cas3. Mol. Cell *46*, 595–605.

Wiedenheft, B., van Duijn, E., Bultema, J.B., Waghmare, S.P., Zhou, K., Barendregt, A., Westphal, W., Heck, A.J., Boekema, E.J., Dickman, M.J., and Doudna, J.A. (2011). RNA-guided complex from a bacterial immune system enhances target recognition through seed sequence interactions. Proc. Natl. Acad. Sci. USA *108*, 10092–10097.

Yosef, I., Goren, M.G., and Qimron, U. (2012). Proteins and DNA elements essential for the CRISPR adaptation process in *Escherichia coli*. Nucleic Acids Res. *40*, 5569–5576.

Zhang, J., Rouillon, C., Kerou, M., Reeks, J., Brugger, K., Graham, S., Reimann, J., Cannone, G., Liu, H., Albers, S.V., et al. (2012). Structure and mechanism of the CMR complex for CRISPR-mediated antiviral immunity. Mol. Cell *45*, 303–313.

Cell

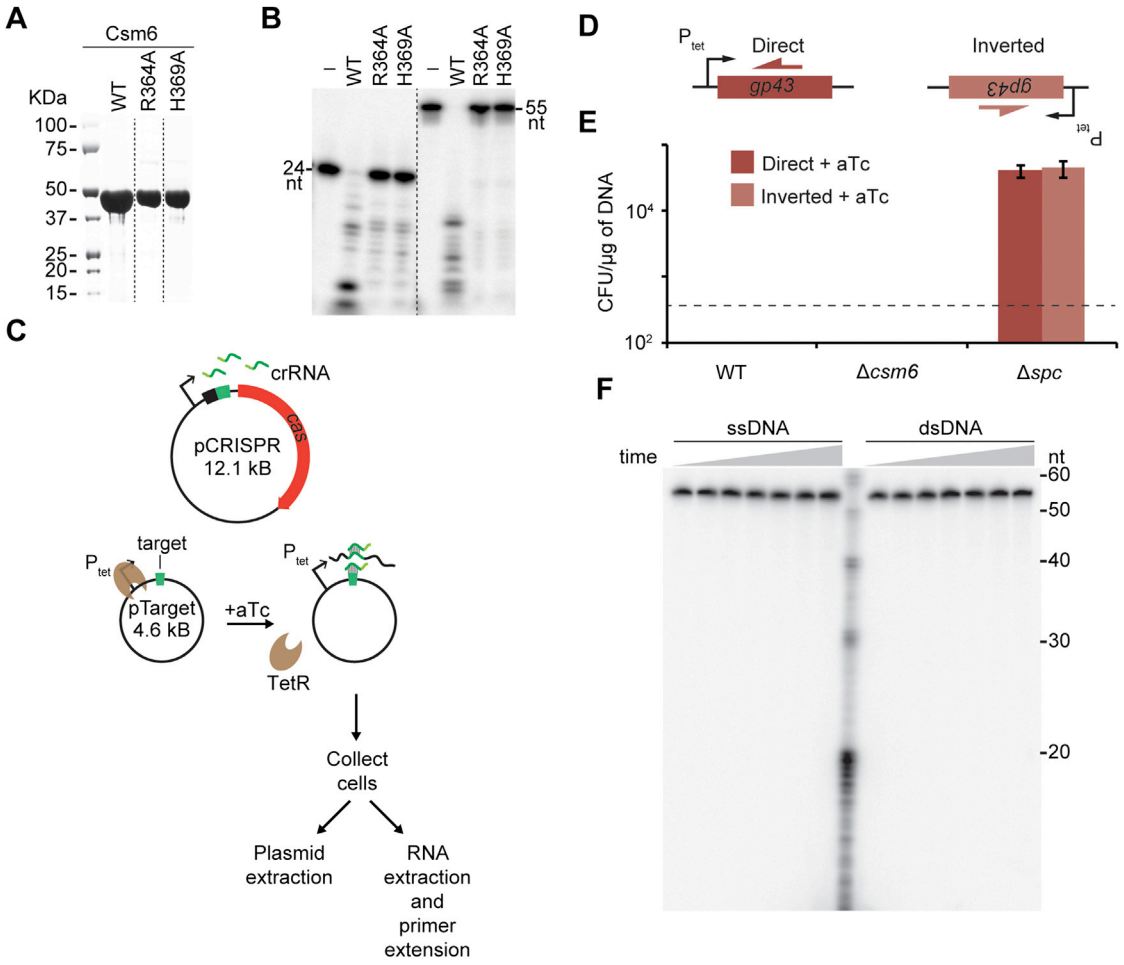

Figure S1. Csm6 Is Not Required for Chromosomal Targeting, Related to Figure 1

(A) Csm6 purification. SDS-PAGE of *S. epidermidis* Csm6 and its putative active site mutants, R364A and H369A purified from *E. coli*.

(B) RNase activity assay for Csm6. The wild-type and mutant purified enzymes were incubated with two different 5′ radiolabeled ssRNA substrates of 24 and 55 nucleotides in length (R24 and R55, respectively, in Table S2). (-) indicates the control without enzyme added.

(C) Inducible anti-plasmid CRISPR immunity assay. Staphylococci are transformed with two plasmids: pCRISPR carrying the type III-A CRISPR-Cas system of *S. epidermidis* and pTarget harboring the target under the control of the tetracycline-inducible promoter P_{tet}. In the absence of the anhydro-tetracycine inducer (aTc) the tetracycline repressor (TetR) prevents *nes* transcription and therefore CRISPR immunity against pTarget. Addition of aTc triggers immunity, and the fate of pTarget and its transcripts over time can be followed by plasmid extraction and RNA extraction and primer extension, respectively.

(D) The *gp43* target from phage ΦNM1γ6 was inserted into the *geh* locus of *S. aureus* RN4220, under the control of a tetracycline-inducible promoter, P_{tet}. The target was placed in both orientations with respect to the origin of replication (direct and inverted insertions); the sequence complementary to the crRNA is either in the leading or lagging strand.

(E) Competent cells containing these targets were transformed with pCRISPR-Cas plasmids carrying wild-type, Δ*csm6* or Δ*spc* (non-targeting control) type III-A systems and plated in the presence of the aTc inducer. Co-transcriptional cleavage of the target DNA prevents colony formation, presumably through the introduction of lethal chromosomal lesions, and results in low transformation efficiencies. Transformation efficiency was measured as the number of colony-forming units (cfu) per µg of plasmid DNA (mean ± SD of three replicas). The dotted line indicates the limit of detection of the assay.

(F) DNase activity assay for wild-type Csm6. The enzyme was incubated either with a 5′ radiolabeled ssDNA oligonucleotide (PS362, Table S2) or dsDNA substrate obtained by annealing PS362 and PS363 (Table S2). The reaction proceeded for 2 hr and aliquots were taken at 0, 15, 30, 45, 60, 90 and 120 min for PAGE and phosphorimager visualization.

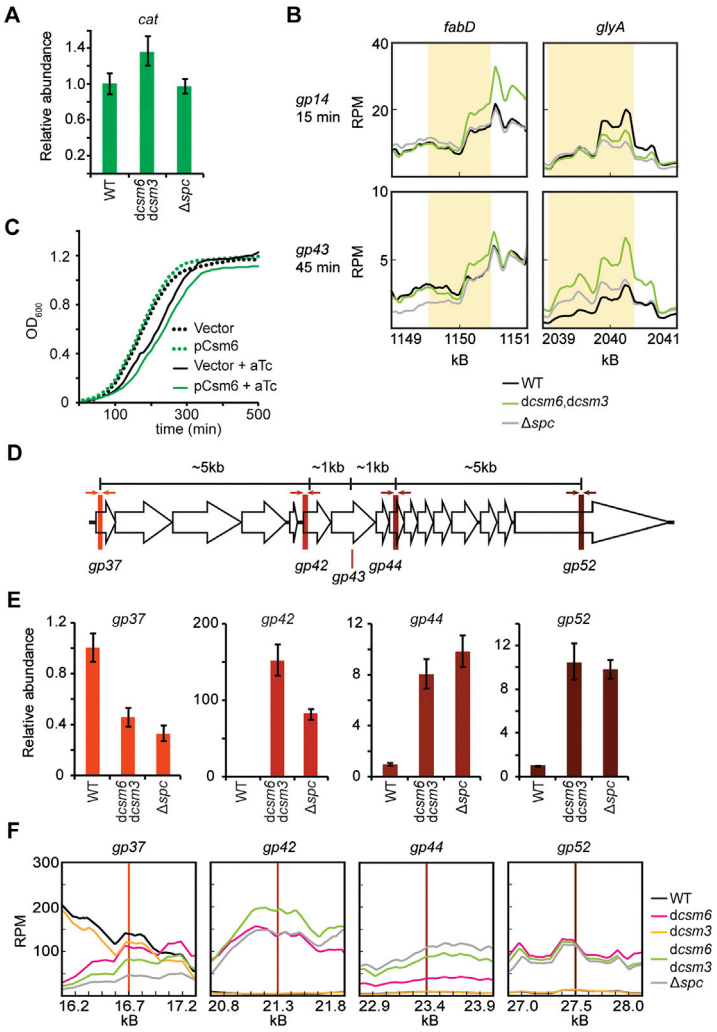

Figure S2. Csm6 and Csm3 Degrade Phage RNA in the Vicinity of the Region Targeted by the Cas10-Csm Complex, Related to Figure 2

(A) RT-qPCR performed on the cellular (non-phage, carried by the pCRISPR-Cas plasmid) chloramphenicol acetyl transferase (*cat*) transcript using total RNA collected at 45 min after infection with ΦNM1γ6 of cells carrying different type III-A CRISPR-Cas systems targeting the *gp43* gene: wild-type, double RNase mutant (d*csm6*/d*csm3*) and a non-targeting control (Δ*spc*). Values for the *rho* gene were used for normalization to obtain the relative abundance of the *cat* transcript for each data point (mean ± SD of four replicas).

(B) RNA-seq reads (Reads Per 500 bases of transcript per Million mapped reads, RPM) for transcripts of the *fabD* (a malonyl CoA-acyl carrier protein transacylase essential for fatty acid biosynthesis) and *glyA* (a serine hydroxymethyltransferase involved in different biosynthetic pathways) housekeeping genes during CRISPR immunity against ΦNM1γ6 infection. RPM values for the open reading frame of these genes (highlighted in yellow) during CRISPR targeting of the *gp14* or *gp43* genes at 15 and 45 min post-infection are shown. Transcript levels in wild-type, double RNase mutant (d*csm6*/d*csm3*) and non-targeting (Δ*spc*) cells are shown.

(C) Growth of staphylococci during overexpression of Csm6. The *csm6* gene was cloned into the pE194 plasmid (empty vector control) under the control of a tetracycline-inducible promoter. Both plasmids were transformed into *S. aureus* RN4220 and selected transformants were grown in the presence or absence of the transcription inducer aTc. Optical density at 600 nm (OD_{600}) was measured for 8 hr to monitor cell toxicity due to overexpression of Csm6. Representative growth curves of at least three independent assays are shown.

(D) Detailed map of the genomic region of phage ΦNM1γ6 harboring the *gp43* gene. The distance from *gp43* of different transcripts assayed by RT-qPCR in (E) are shown. The opposed arrows indicate the primers used for these RT-qPCR experiments.

(E) Same as (A) but measuring phage transcripts *gp37*, *gp42*, *gp44* and *gp52*. In the vicinity of the target, either 1 kb upstream (*gp42*) or downstream (*gp44*), phage mRNA accumulated in d*csm3*/d*csm6* cells to similar levels of cells without type III-A immunity against the phage (Δ*spc*). We observed a similar accumulation further downstream (*gp52*, 5 kb from the *gp43* target), but not further upstream, where *gp37* transcript abundance in wild-type, d*csm3*/d*csm6* and Δ*spc* was not significantly different. This result suggests that Csm6 has a preference for degrading transcripts in the vicinity of the target region (at least within 1 kb) as well as downstream of it.

(F) Same as (B) but measuring phage transcripts levels across the *gp37*, *gp42*, *gp44* and *gp52* targets in wild-type, double RNase mutant (d*csm6*/d*csm3*), single d*csm3* and d*csm6* mutants and non-targeting (Δ*spc*) cells. Colored vertical lines indicate target positions.

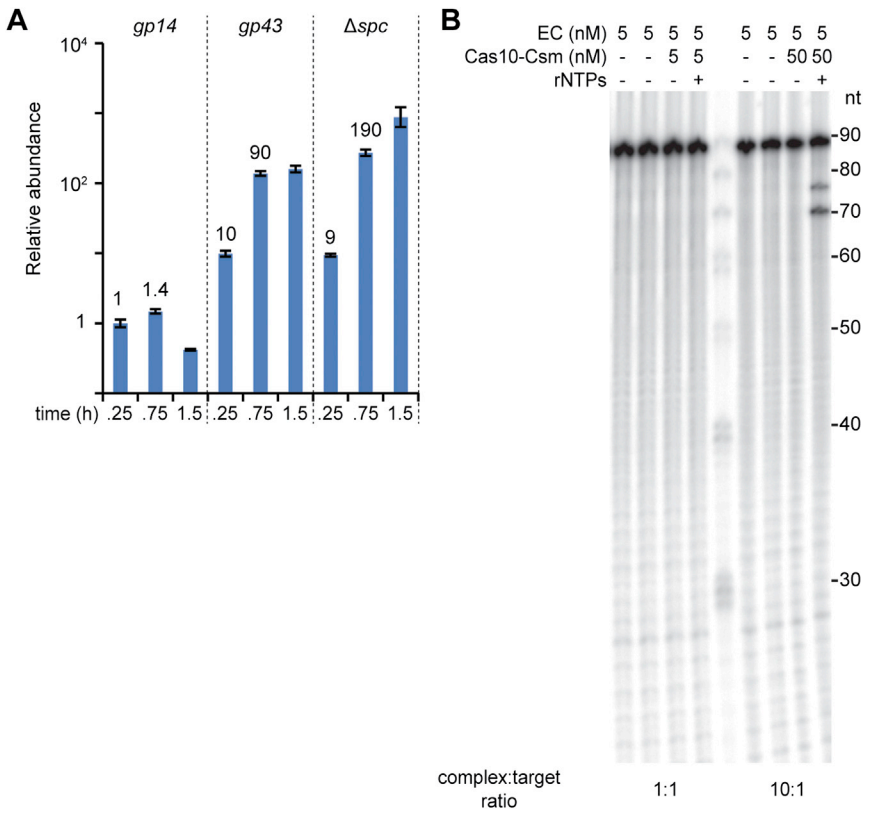

Figure S3. Accumulation of the *gp14* Phage DNA during Targeting of the *gp43* ΦNM1γ6 Gene, Related to Figure 3

(A) Same as Figure 3D but performing qPCR with primers specific for the amplification of the *gp14* gene. qPCR was performed on this gene using total DNA collected at different times post-infection from cells carrying different CRISPR-Cas systems: type III-A targeting the *gp14* gene, type III-A targeting the *gp43* gene and a non-targeting type III-A control (Δ*spc*). Values for the *rho* gene were used for normalization to obtain the relative abundance of the *gp14* gene for each data point (mean ± SD of four replicas).

(B) Co-transcriptional DNA cleavage of the Cas10-Csm complex at different complex:target ratio. 5 nM of elongation complexes containing a radiolabeled dsDNA *nes* target and RNA polymerase (EC) were incubated with 5 and 50 nM of purified Cas10-Csm complex harboring a crRNA guide matching the *nes* target. rNTPs were added to initiate transcription and the products of the reactions (30 min after addition of rNTPs) were subject to PAGE and phosphorimager visualization.

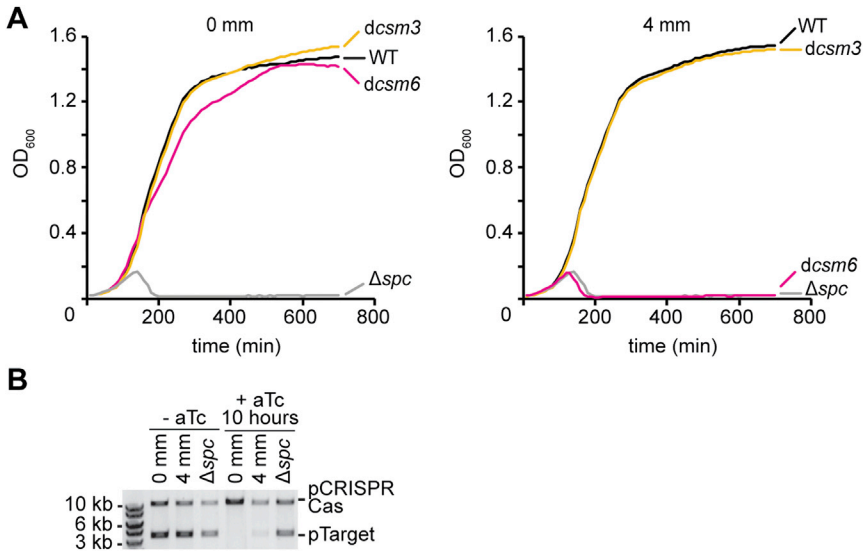

Figure S4. Contribution of the Csm3 and Csm6 Active Sites to Type III-A CRISPR-Cas Immunity in the Presence of crRNA:target Mismatches, Related to Figure 6

(A) Staphylococci harboring different type III-A CRISPR-Cas systems targeting the *gp43* gene were grown in liquid media and infected with ϕNM1γ6 phage (at 0 hr) with a multiplicity of infection of 5 viruses per bacteria. The different genetic backgrounds were wild-type, inactive Csm6 RNase (d*csm6*), inactive Csm3 RNase (d*csm3*) and a non-targeting control (Δ*spc*), expressing a crRNA with either 4 or no mismatches (4 mm or 0 mm) with the *gp43* target. Optical density at 600 nm (OD_{600}) was measured for the following 12 hr to monitor cell survival due to CRISPR immunity against the phage.

(B) Plasmid DNA degradation in the presence or absence of crRNA:target mismatches. pTarget plasmid DNA, harboring the *gp43* target under the control of a tetracycline-inducible promoter, was extracted from cells harboring a type III-A CRISPR-Cas system without a spacer (Δ*spc*) or with a gp43-targeting spacer with or without mismatches (4 mm or 0 mm, respectively), either before or after 10 hr of treatment with aTc. Plasmid DNA was visualized by agarose gel electrophoresis followed by ethidium bromide staining.

Cell, Volume *164*

Supplemental Information

Degradation of Phage Transcripts by CRISPR-Associated RNases Enables Type III CRISPR-Cas Immunity

Wenyan Jiang, Poulami Samai, and Luciano A. Marraffini

Supplemental Experimental Procedures

Cloning in *E.coli*

Cloning used *E.coli* DH5α electrocompetent cells. To clone WT Csm6 for purification, PCR was performed using pWJ30β (Hatoum-Aslan et al., 2013) as template and primers PS11 and PS12. The PCR product was digested with restriction enzymes NdeI and XhoI and ligated to the vector pET23a-His_6(C-terminal) digested with the same enzymes, making plasmid pPS10. The Csm6 mutants R364A (plasmid pPS42), H369A (plasmid pPS43) and R364A-H369A (plasmid pPS44) were constructed using the plasmid pPS10 as a backbone with three sets of primers PS245/PS246, PS243/PS244 and PS247/PS248, respectively. The sequences of the primers used in this study are listed in Supplemental Table S2.

Cloning in *S. aureus*

Cloning used *S. aureus* RN4220 electrocompetent cells. For type III-A pCRISPR-Cas plasmids, new spacers were cloned by ligation of annealed oligonucleotide pairs and BsaI-digested parent vector, pGG-BsaI-R (Goldberg et al., 2014). The sequences of the spacers cloned for this study is in Supplemental Table S1. To construct Δ*csm6* plasmids, PCR was performed using WT plasmid as template and primers L342/L343. PCR product was restriction digested with PspOMI and EagI (NEB), followed by ligation by T4 DNA Ligase (NEB). To construct d*csm6* plasmids, PCR was performed using WT plasmid as template and primers W852/PS248 and primers PS247/W614. The two PCR products were then ligated using Gibson assembly (Gibson et al., 2009). To construct d*csm3* plasmids, PCR was performed using WT plasmid as template and primers W852/PS466 and primers PS465/W614. The two PCR products were then ligated using Gibson assembly. To construct pCsm6 overexpression plasmid, one PCR was performed using pWJ153 (Goldberg et al., 2014) as template and primers W1129/W1113. Another PCR was performed using pWJ30β as template and primers W1127/W1128. The two PCR products were then ligated using Gibson assembly. The sequences of the primers used in this study are listed in Supplemental Table S2.

Purification of Csm6

The pPS10, pPS42, pPS43 and pPS44 plasmids were transformed into *E. coli* BL21 (DE3) Rosetta 2 cells (Merck Millipore). Cultures (1 liter) were grown at 37 °C in Terrific Broth medium (Fisher Scientific) containing 100 µg/ml ampicilin and 34 µg/ml chloramphenicol until the OD_{600} reached 0.6. The cultures were adjusted to 0.3 mM isopropyl-1-thio-β-d-galactopyranoside and incubation was continued for 16 h at 16 °C with constant shaking. The cells were harvested by centrifugation and the pellets stored at −80 °C. All subsequent steps were performed at 4 °C. Thawed bacteria were resuspended in 35 ml of buffer A (50 mM Tris–HCl, pH 7.5, 500 mM NaCl, 200 mM Li_2SO_4, 20% sucrose, 15 mM Imidazole) containing one complete EDTA free protease inhibitor tablet (Roche).

Triton X-100 and lysozyme were added to final concentrations of 0.1 % and 0.1 mg/ml, respectively. After 1 hour, the lysate was sonicated to reduce viscosity. Insoluble material was removed by centrifugation for 1 hour at 15,000 rpm in a Beckman JA-3050 rotor. The soluble extract was mixed for 1 hour with 5 ml of Ni^{2+}-Nitrilotriacetic acid-agarose resin (Thermo) that had been pre-equilibrated with buffer A. The resin was recovered by centrifugation, then first washed with 50 ml of buffer A, followed by washing with 50 ml of IMAC buffer (50 mM Tris-HCl pH 7.5, 250 mM NaCl, 10% glycerol) containing 50 mM imidazole. The resin was subsequently resuspended in 10 ml of IMAC buffer containing 100 mM imidazole, and then poured into a column. The column was then eluted step-wise with 10 ml aliquots of IMAC buffer (50 mM Tris-HCl pH 7.5, 250 mM NaCl, 10% glycerol) containing 200, and 500 mM imidazole. The 500 mM imidazole elutes containing the protein was pooled together and dialyzed against 50 mM Tris-HCl pH 7.5, 50 mM NaCl, 10% glycerol. Subsequently Csm6 was purified using a 5 ml HiTrap Q Sepharose Fast Flow (GE Life Sciences), eluting with a linear gradient of 50 mM - 2 M NaCl. The peak fraction from the Q sepharose column was further purified by hydrophobic interaction chromatography using butyl sepharose 4 FF (GE Healthcare Life Sciences), eluting with stepwise lowering of ammonium sulphate concentration from 1 M to 50 mM. The final purification step was performed using size exclusion chromatography with *Superdex 200 10/300 GL* (GE Healthcare) column, using buffer B (50 mM Tris-HCl pH 7.5, 5% glycerol, 150 mM NaCl, 1 mM TCEP).

Transcription Coupled DNA Cleavage

Elongation complexes (ECs) were reconstituted essentially as described in (Samai et al., 2015). Typically, 2 µl 1 pmol/µl of template strand (TS) and 1 µl of 4 pmol/µl RNA oligos were mixed in 1 × transcription buffer and incubated at 65°C for 5 min, followed by gradual cooling to room temperature. After addition of 1.5 µl *E. coli* RNAP core enzyme (NEB), the reaction was incubated at 25°C for 25–30 min and at 37°C for 1 min. Then, 4 µl 1.25 pmol/µl nontemplate strand (NTS) (pretreated by heating to 65°C for 5 min, then on ice for 2 min, and finally at 37°C for 2 min) was added and incubated for 10–15 min at 37°C. The final concentration of TS was 0.10 pmol/µl after adding supplement buffer to obtain transcription conditions. Assembled ECs were kept on ice until use. In a transcription coupled DNA cleavage assay, 5 nM of EC was used and, Cas10-Csm complex was added to a final concentration of 5 nM and 50 nM. Transcription was initiated with the addition of 2.5 mM of RNTPs. All the reactions were performed at 37°C. For all the DNA cleavage time course experiments, RNTPs were added to the elongation complex (EC), prior to the addition of Cas10-Csm complex. After addition of Cas10-Csm, the samples were collected at 30 min, and quenched by mixing with Proteinase K (NEB) and 20 mM EDTA. The DNA/RNA samples were then extracted using phenol-chloroform-isoamyl alcohol (25:24:1), ethanol precipitated and resuspended into loading buffer (90% formamide). The DNA products were heater at 95°C for 5 min before loading onto the gel. Cleavage products were resolved on a 12%

denaturing polyacrylamide gels containing 7 M urea and visualized by phosphorimaging (Typhoon, GE Life Sciences).

Phage infections and plate reader growth curves

Cells were infected during early log phase (at OD_{600} of 0.3-0.4). Plate reader growth curves were measured as previously described with slight modifications. Briefly, overnight cultures were launched from single colonies and diluted 1:250 in TSB broth supplemented with 5mM $CaCl_2$ and appropriate antibiotics. After 1 h of growth, phage was added at a multiplicity of infection (MOI) of 5. Measurements were taken every 10 minutes.

Total RNA Extraction

10-25 ml of *S. aureus* culture were pelleted and immediately frozen at -20°C. Pellets were gently thawed at 4°C and washed with 1 ml ice-cold TE pH 6.8. Pellets were re-suspended in 100 µl of ice-cold TE pH 6.8 and mixed with 750 µl of ice-cold TRIzol®. The mix was transferred into a 2 ml microtubes pre-filled with 0.25 cm^3 of 0.1 mm glass beads on ice. Cells were disrupted using Mini-Beadbeater-1 (BioSpec Products) at an intensity setting of 42 for 30 seconds twice at 4°C. 200 µl of chloroform was added to the disrupted mix was and the rest of RNA extraction protocol was followed according to TRIzol®.

Total DNA Extraction

10-25 ml of *S. aureus* culture were pelleted and immediately frozen at -20°C. Pellets were gently thawed at 4°C and washed with 1 ml ice-cold TE pH 8.0. Pellets were re-suspended in 400 µl of ice-cold TE pH 8.0 and mixed with 500 µl of ice-cold Phenol/Chloroform/Isoamyl alcohol (25:24:1) (Fisher Scientific). The mix was transferred into a 2 ml microtubes pre-filled with 0.25 cm^3 of 0.1 mm glass beads on ice. Cells were disrupted using Mini-Beadbeater-1 (BioSpec Products) at an intensity setting of 42 for 30 seconds twice at 4°C. The disrupted mix was centrifuged at 16,000 rcf for 10 minutes at room temperature. The aqueous phase was collected and mixed with 500 µl of chloroform and centrifuged as above. The aqueous phase was collected again and mixed with 1 ml of isopropanol. Precipitated DNA was washed with 1 ml of 75% ethanol, air dried and dissolved in 50-300 µl of water.

Plasmid-curing assay

RN4220 cells harbouring both the WT CRISPR-Cas plasmid or its variant and the pWJ153 target plasmid were cultured in TSB supplemented with chloramphenicol (10 µg/ml). ATc was added to a final concentration of 0.25 µg/ml during log phase (at OD_{600} of 0.6-0.8). Plasmid DNA was prepared at designated time points, linearized with the common single cutter BamHI and subjected to agarose gel electrophoresis.

Supplemental references

Gibson, D.G., Young, L., Chuang, R.Y., Venter, J.C., Hutchison, C.A., 3rd, and Smith, H.O. (2009). Enzymatic assembly of DNA molecules up to several hundred kilobases. Nat Methods *6*, 343-345.

Goldberg, G.W., Jiang, W., Bikard, D., and Marraffini, L.A. (2014). Conditional tolerance of temperate phages via transcription-dependent CRISPR-Cas targeting. Nature *514*, 633-637.

Hatoum-Aslan, A., Samai, P., Maniv, I., Jiang, W., and Marraffini, L.A. (2013). A ruler protein in a complex for antiviral defense determines the length of small interfering CRISPR RNAs. J Biol Chem *288*, 27888-27897.

Samai, P., Pyenson, N., Jiang, W., Goldberg, G.W., Hatoum-Aslan, A., and Marraffini, L.A. (2015). Co-transcriptional DNA and RNA Cleavage during Type III CRISPR-Cas Immunity. Cell *161*, 1164-1174.

Supplemental tables.

Supplemental Table S1. Spacers used in this study (5'-3'). Related to Fig. 2

ΦNM1γ6 gene targeted	Upstream sequence	Spacer sequence (5'-3')	Downstream sequence
gp5	TTTCG	CCATTCATCTAATTTCAAGGCTATGTTTGATGTAG	-
gp14	TTCTA	CTACGTCCGTAATGCTAGGATTTGCAAATTTCTTA	-
gp19	TTCTA	CACCCATATCATCTAGTACAAGTAAATCAATATCA	-
gp32	CATAC	GTAAACCTTTGATTGCTCTTAGCTCGAGTTATGTGC	-
gp43	TTCTA	ATTCGTCATCTTCAAGTAATGCCTCTAAATCAATA	-
gp43 (3 mm)	TTCTA	TTTCGTCTTCTTCATGTAATGCCTCTAAATCAATA	-
gp43 (4 mm)	TTCTA	TTTCGTCATCTTCATGTAATGCCTCTAAATCAATA	-
gp43 (5 mm)	TTCTA	TTTGGTCATCTTCATGTAATGCCTCTAAATCAATA	-
gp43 (type II)	-	ACTTCACACAAGATAACATTATTGATTTAG	AGGCA
gp50	TTCTA	GTCCAATATTTTCTGCGATTTCATCTAGTGCTTCA	-
gp59	TTCTA	ATCGCGTTAAACGCCAATCTTGTTCGTGTCGTTTG	-

Supplemental Table S2. DNA Oligonucleotides used in this study (5'-3').
Related to Supplemental Experimental procedures.

Name	Sequence (5'-3')	Purpose
A248	CCTCCTTATAAAATTAGTATAATTATAGCAC	Primer extension
L342	aaaGGGCCCAAATAATATTTTCATTATAGCACCTC	Cloning of Δ*csm6*
L343	aaaCGGCCGGAAAAAAATAAGGAATTTAAAGAGC	Cloning of Δ*csm6*
PS11	CGCCATATGAAAATATTATTTAGTCCAATAGG	Cloning of Csm6
PS12	CGCCTCGAGTAATAGCTCTTTAAATTCC	Cloning of Csm6
PS243	GGTTTAAGAAATTCCATAGCCGCTAATTTAGATAC	Cloning of Csm6 (H369A)
PS244	GTATCTAAATTAGCGGCTATGGAATTTCTTAAACC	Cloning of Csm6 (H369A)
PS245	CGATATAAATGGTTTAGCAAATTCCATAGCCC	Cloning of Csm6 (R364A)
PS246	GGGCTATGGAATTTGCTAAACCATTTATATCG	Cloning of Csm6 (R364A)
PS247	GATATAAATGGTTTAGCAAATTCCATAGCCGCTAATTTAGATAC	Cloning of Csm6(R364A, H369A)
PS248	GTATCTAAATTAGCGGCTATGGAATTTGCTAAACCATTTATATC	Cloning of Csm6(R364A, H369A)
PS362	GTATAGGCACAGCGGGAATAAGGCTATCACTGATGTGCTCGAGTAACTTAACAGC	DNA cleavage assay
PS363	GCTGTTAAGTTACTCGAGCACATCAGTGATAGCCTTATTCCCGCTGTGCCTATAC	DNA cleavage assay
PS465	GAATCTAGTATGATTGGAGCAATTGcTTCTCCTGTAGTTAGAGATTTGCAAACC	Cloning of Csm3(D32A)
PS466	GGTTTGCAAATCTCTAACTACAGGAGAAgCAATTGCTCCAATCATACTAGATTC	Cloning of Csm3(D32A)
W176	CCTATCTGACAATTCCTGAATAG	*cat* qPCR
W614	GGTTATACTAAAAGTCGTTTGTTGG	Cloning
W653	ATTTACCGCTATCTTTACAGGTAC	*cat* qPCR
W852	CCAACAAACGACTTTTAGTATAACC	Cloning
W863	TATGTGGCCGAAAAAACCAAGC	Probe for southern blot
W864	TTGGATATCCATAGTTTTTACACC	Probe for southern blot
W865	ATGACATCAGAAGCGGTTGACG	Probe for southern blot
W866	TGGTTTAACAGTGCGTCTAATCC	Probe for southern blot
W893	TCCATTCGGTAAATCAATTGCAC	*gp43* qPCR
W894	TGTTTTTGAGATAAACGCATTTGC	*gp43* qPCR
W897	GAAGAATCAGATGGAGATAATGG	*gp42* qPCR
W898	AAGACGCTTGTTATATTCTTCTTG	*gp42* qPCR
W901	TGCAGTTAAACGCTACAACAGG	*gp44* qPCR
W902	CTTCATACTCCTTGAAATCGTTC	*gp44* qPCR
W905	TTATAGTAAGAAAACAGCAGAGTC	*gp37* qPCR
W906	AAACGCTCTTCTTGTATCTGTTC	*gp37* qPCR
W909	TGAATGCATTCAGCGGATCATC	*gp52* qPCR
W910	GATTGTCCAACTTGTTCAGACC	*gp52* qPCR
W915	GTCAATGACCATAACGCAGAAG	*rho* qPCR
W916	CAATCGGTGTTACTAAATCCATG	*rho* qPCR
W1085	GATTAGACATTCACCTTCAATAAC	*gp14* qPCR
W1086	TTGCGCTTGTCCTGTGATTTTC	*gp14* qPCR
W1113	TATGAGATAATGCCGACTGTACTTTTTACAGTCGGTATCAGAGCTCGTGCTATAATT	Cloning of pCsm6
W1127	GCTCTCTATCATTGATAGAGTGAGTTAAACAATGAGGTGCTATA*A*TG	Cloning of pCsm6
W1128	GTAAAAAGTACAGTCGGCATTATCTCATATTTATCATAATAGCTCTTTAAATTCC	Cloning of pCsm6
W1129	TCACTCTATCAATGATAGAGAGC	Cloning of pCsm6

Supplemental Table S3. RNA oligonucleotides used in this study (5'-3'). Related to Supplemental Experimental procedures.

Name	Sequence
R24	CGUGUCGCCCUUAUUCCGAUAGUG
R55	GCUGUUAAGUUACUCGAGCACAUCAGUGAUAGCCUUAUUCCCGCUGUGCCUAUAC